Organization of the Multiple Coenzymes and Subunits and Role of the Covalent Flavin Link in the Complex Heterotetrameric Sarcosine Oxidase†

Michel Eschenbrenner, Lawrence J. Chlumsky, Peeyush Khanna, Francoise Strasser, and Marilyn Schuman Jorns*

Department of Biochemistry, MCP Hahnemann School of Medicine, Philadelphia, Pennsylvania 19129

Received January 16, 2001; Revised Manuscript Received March 2, 2001

ABSTRACT: Heterotetrameric ($\alpha\beta\gamma\delta$) sarcosine oxidase from *Corynebacterium* sp. P-1 (cTSOX) contains noncovalently bound FAD and NAD^+ and covalently bound FMN, attached to β(His173). The β(His173Asn) mutant is expressed as a catalytically inactive, labile heterotetramer. The β and δ subunits are lost during mutant enzyme purification, which yields a stable $\alpha\gamma$ complex. Addition of stabilizing agents prevents loss of the δ but not the β subunit. The covalent flavin link is clearly a critical structural element and essential for TSOX activity or preventing FMN loss. The α subunit was expressed by itself and purified by affinity chromatography. The α and β subunits each contain an NH_2-terminal ADP-binding motif that could serve as part of the binding site for NAD^+ or FAD. The α subunit and the $\alpha\gamma$ complex were each found to contain 1 mol of NAD^+ but no FAD. Since NAD^+ binds to α, FAD probably binds to β. The latter could not be directly demonstrated since it was not possible to express β by itself. However, FAD in TSOX from *Pseudomonas maltophilia* (pTSOX) exhibits properties similar to those observed for the covalently bound FAD in monomeric sarcosine oxidase and *N*-methyltryptophan oxidase, enzymes that exhibit sequence homology with β. A highly conserved glycine in the ADP-binding motif of the α(Gly139) or β(Gly30) subunit was mutated in an attempt to generate NAD^+- or FAD-free cTSOX, respectively. The α(Gly139Ala) mutant is expressed only at low temperature ($t_{optimum}$ = 15 °C), but the purified enzyme exhibited properties indistinguishable from the wild-type enzyme. The much larger barrier to NAD^+ binding in the case of the α(Gly139Val) mutant could not be overcome even by growth at 3 °C, suggesting that NAD^+ binding is required for TSOX expression. The β(Gly30Ala) mutant exhibited subunit expression levels similar to those of the wild-type enzyme, but the mutation blocked subunit assembly *and* covalent attachment of FMN, suggesting that both processes require a conformational change in β that is induced upon FAD binding. About half of the covalent FMN in recombinant preparations of cTSOX or pTSOX is present as a reversible covalent 4a-adduct with a cysteine residue. Adduct formation is not prevented by mutating any of the three cysteine residues in the β subunit of cTSOX to Ser or Ala. Since FMN is attached via its 8-methyl group to the β subunit, the FMN ring must be located at the interface between β and another subunit that contains the reactive cysteine residue.

Heterotetrameric sarcosine oxidase (TSOX)[1] is a sarcosine-inducible bacterial enzyme that is important in the catabolism of sarcosine (*N*-methylglycine), a common soil metabolite that can act as sole source of carbon and energy for many microorganisms (*1*). TSOX is a complex, multimeric enzyme that catalyzes both sarcosine oxidation and the synthesis of 5,10-methylenetetrahydrofolate (5,10-CH_2-H_4folate). TSOX contains four different subunits (α, β, γ, δ) that range in size from about 100 to 10 kDa (103, 44, 21, and 11 kDa, respectively). The isolated enzyme contains three coenzymes (noncovalently bound FAD and NAD^+ and covalently bound FMN) and a binding site for a fourth coenzyme [tetrahydrofolate (H_4folate)] that acts as a substrate (*2*−*7*). TSOX contains a single binding site for sarcosine near the noncovalently bound FAD. Sarcosine oxidation to the corresponding imine is accompanied by the reduction of FAD to 1,5-dihydroFAD ($FADH_2$). Electrons from $FADH_2$ are transferred, one at a time, to the covalently bound FMN, which then reduces oxygen to hydrogen peroxide (*8*, *9*) (Scheme 1). In the absence of H_4folate, the sarcosine imine is hydrolyzed to yield glycine and formaldehyde. In the presence of H_4folate, TSOX catalyzes the transfer of the oxidized 1-carbon fragment from the imine to H_4folate, forming 5,10-CH_2-H_4folate plus glycine (*6*, *7*). The role of NAD^+ is unknown.

The 8α-position of the FMN ring is attached to N(3) of His173 in the β subunit of TSOX from *Corynebacterium* sp. P-1 (*5*). An additional covalent link is found in the recombinant enzyme where about half of the covalent FMN

† This work was supported in part by Grant GM 31704 (M.S.J.) from the National Institutes of Health.

* To whom correspondence should be addressed. Phone: (215) 991-8580. Fax: (215) 843-8849. E-mail: marilyn.jorns@drexel.edu.

[1] Abbreviations: TSOX, heterotetrameric sarcosine oxidase; cTSOX, TSOX from *Corynebacterium* sp. P-1; pTSOX, TSOX from *Pseudomonas maltophilia*; aTSOX, TSOX from *Arthrobacter* sp. 1-IN; FAD, flavin adenine dinucleotide; MSOX, monomeric sarcosine oxidase; MTOX, *N*-methyltryptophan oxidase; FMN, flavin adenine mononucleotide; EDTA, ethylenediaminetetraacetic acid; NAD^+, nicotinamide adenine dinucleotide; SDS−PAGE, sodium dodecyl sulfate−polyacrylamide gel electrophoresis; IPTG, isopropyl β-D-thiogalactopyranoside; SHMT, serine hydroxymethyltransferase; TCA, trichloroacetic acid; MMTS, methyl methanethiosulfonate; MTA, methylthioacetate.

10.1021/bi010101p CCC: $20.00
Published on Web 04/13/2001

Scheme 1: Sarcosine Oxidation by TSOX in the Presence and Absence of H_4folate

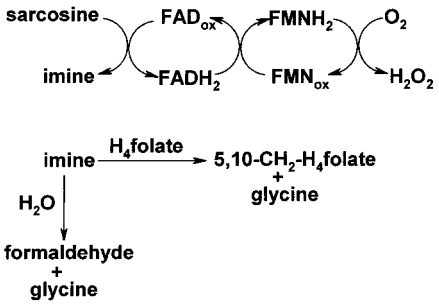

forms a reversible 4a-adduct with an unidentified cysteine residue. Adduct formation is accompanied by changes in the visible absorption spectrum and the appearance of a pronounced lag in an NADH or horseradish peroxidase coupled assay (*10*). The 4a-thiolate adduct is disrupted by reagents that alkylate (methyl methanethiosulfonate, MMTS) or oxidize (H_2O_2) the cysteine residue (Scheme 2). The adduct is not found in the natural enzyme isolated from *Corynebacterium* sp. P-1, probably because the adduct is disrupted in vivo by reaction with H_2O_2 produced during turnover with sarcosine which is used to induce expression of the natural enzyme but not recombinant TSOX (*10*). The location of the binding sites for the other coenzymes and the organization of the multiple subunits are unknown. The α and β subunits, however, contain an NH_2-terminal ADP-binding motif that could serve as part of the binding site for FAD or NAD^+ (*10*).

TSOX is a member of a recently recognized flavoprotein family of amine oxidases. Unlike TSOX, other known members of this family are simple monomeric proteins about 44 kDa in size, contain covalently bound FAD as their only prosthetic group, and do not use H_4folate as a substrate. Other family members include monomeric sarcosine oxidase (MSOX), *N*-methyltryptophan oxidase (MTOX), and pipecolate oxidase (*11*−*16*). The crystal structure of free MSOX and its complexes with substrate analogues has recently been determined (*11*, *14*). The β subunit of TSOX exhibits 23% amino acid sequence identity with MSOX. Residues in MSOX which have been implicated in sarcosine binding and oxidation are conserved in the β subunit of TSOX. The role of the covalent flavin link has not been established for any member of this family.

Most of the studies described in this paper have been conducted with TSOX from *Corynebacterium* sp. P-1 (cTSOX); others have been performed with a recently characterized TSOX from *Pseudomonas maltophilia* (pTSOX). In this paper we show that the covalent flavin link is a critical structural element in TSOX and provide considerable insight regarding the organization of the multiple coenzymes and subunits in this complex enzyme.

EXPERIMENTAL PROCEDURES

Materials. Plasmids pET17b and pET23a were from Novagen. Plasmids pLCJ305 and pLJC400 contain the complete cTSOX operon and are nearly identical pBluescript II SK(+) derivatives except that a *Kpn*I site has been eliminated from the vector DNA in pLJC400; plasmid pLJC305ΔKpnI is a pLJC305 derivative containing a portion of the cTSOX operon (*5*, *10*). Plasmid pBluescript II SK(+)ΔKpnI was constructed as previously described (*5*). *Escherichia coli* strain XL-1 Blue was obtained from Stratagene. Carbenicillin, IPTG, FMN, FAD, TCA, MMTS, yeast alcohol dehydrogenase, horseradish peroxidase, *o*-dianisidine, and imidazole hydrochloride were from Sigma. Sarcosine and methylthioacetic acid were obtained from Aldrich. Sodium sulfite was from Fluka. Glycerol was purchased from Fisher. Tryptone and yeast extracts were from Difco. T4 DNA ligase and the Klenow fragment of DNA polymerase were obtained from New England Biolabs. Restriction enzymes were purchased from New England Biolabs and Promega. Oligonucleotides were purchased from Ransom Hill Bioscience, Inc. The T7 Sequenase version 2.0 DNA sequencing kit was purchased from Amersham Life Science, and sequencing was performed using dITP mixes. The Geneclean II kit was obtained from BIO101. *Taq* DNA polymerase was purchased from Promega and *Pfu* DNA polymerase from Stratagene. dNTPs were from Pharmacia. The Advantage-GC cDNA kit and the Talon affinity resin were purchased from Clontech. Geneluter spin columns were purchased from Supelco. Amicon-10, Microcon-30, and Micropure-EZ columns were obtained from Amicon. The Qiaquick PCR purification kit, Qiaquick gel extraction kit, Qiaprep spin miniprep kit, and midiprep kit were from Qiagen.

PCR. All reactions were performed in a Hybaid Touchdown thermocycler. Unless otherwise indicated, reaction conditions were as specified by the polymerase supplier. PCR fragments were purified by agarose gel (0.8−3%) electrophoresis and recovered using Geneluter spin columns or the Qiaquick gel extraction kit. If required in double restriction digests, the buffer was exchanged and the first restriction enzyme removed using Micropure-EZ in conjunction with a Microcon-30 microconcentrator or a Qiaquick PCR purification kit. After insertion of a PCR fragment into a given vector, the recombinant plasmids were used to transform XL-1 Blue competent cells to ampicillin resistance, unless otherwise indicated. Plasmids from several colonies were

Scheme 2: Reversible Formation of a 4a-Thiolate Adduct in Recombinant TSOX

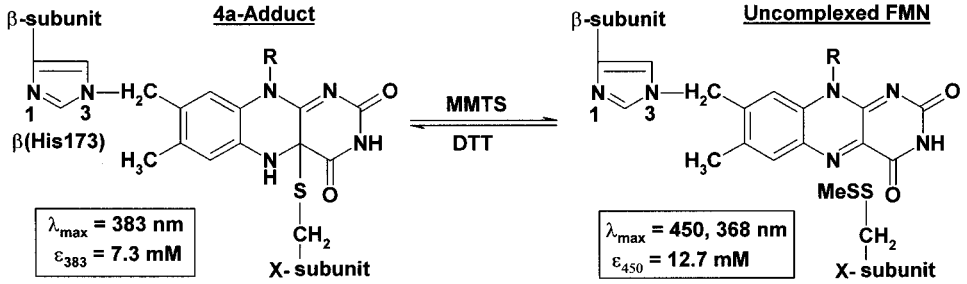

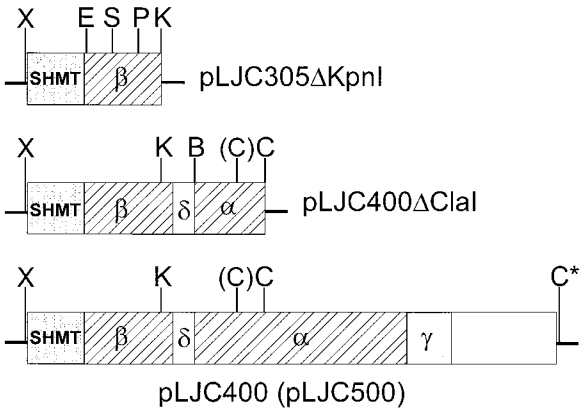

FIGURE 1: Plasmids used in site-directed mutagenesis studies. Vector DNA is shown as a thin line at either end of corynebacterial DNA which contains genes for serine hydroxymethyltransferase (SHMT) and the subunits of cTSOX (β, δ, α, γ), as indicated. Restriction sites are designated as follows: X, *Xba*I; E, *Eco*RI; S, *Sal*I; P, *Pst*I; K, *Kpn*I; B, *Bam*HI; C, *Cla*I; (C), *Cla*I site that is not cut by *Cla*I, probably due to in vivo methylation; C*, *Cla*I site present in pLJC400 but not pLCJ500. Plasmid pLJC305ΔKpnI contains unique restriction sites that flank the codons for β(Gly30) (*Eco*RI, *Sal*I), β(Cys146) (*Sal*I, *Pst*I), β(Cys195) (*Sal*I, *Pst*I), and β(Cys351) (*Pst*I, *Kpn*I). Plasmids pLJC305ΔKpnI and pLJC400 (*5*, *10*) were used as intermediate and final cloning vectors, respectively, in creating mutations at these sites. Plasmid pLJC400ΔClaI contains unique functional restriction sites (*Bam*HI, *Cla*I) that flank the codon for α(Gly139) and was used as the intermediate vector in mutating this residue; pLJC500 was used as the final cloning vector. The construction of pLJC400Δ*Cla*I and pLJC500 is described in Experimental Procedures.

generally initially screened by restriction analysis and then sequenced across the entire insert. Automated DNA sequencing was conducted at the Nucleic Acid/Protein Research Core Facility of Children's Hospital of Philadelphia using Big Dye terminators and the Perkin-Elmer ABI 377 DNA sequencer. In a few cases, manual DNA sequencing was done using the T7 Sequenase version 2.0 DNA sequencing kit and dITP mixes.

Mutagenesis. All site-directed mutations were generated using PCR and the overlap extension method described by Ho et al. (*17*). The large size of the cTSOX operon made it difficult to identify unique restriction sites that flanked codons targeted for mutagenesis. This problem was resolved by using intermediate cloning vectors (pLJC305ΔKpnI, pLJC400ΔClaI), created by deleting a portion of the corynebacterial DNA from pLJC305 or pLJC400, respectively (Figure 1). After a fragment of the wild-type sequence was substituted with the corresponding mutagenic PCR product, the corynebacterial DNA was cut out from the intermediate cloning vector and subcloned into the final cloning vector (pLJC400 or pLJC500). The only difference between pLCJ400 and pLCJ500 is that a *Cla*I site in the vector multicloning region is deleted in pLJC500 (Figure 1).

Reactions for the generation of the β(Cys146Ser) mutation were conducted using pLJC305 as template and 1.25 units of *Pfu* DNA polymerase. For the generation of the β-(Cys195Ser) or β(Gly30Ala) mutation, pLJC305 was used as template with 2.5 units of *Taq* DNA polymerase (Promega) in 1.5 mM $MgCl_2$. Reactions for the generation of the β(Cys351Ala), β(His173Ala), and β(His173Asn) mutations were conducted using 1.25 units of *Pfu* DNA polymerase with pLJC400 as template. As will be described, generation of the α(Gly139Ala) or α(Gly139Val) mutation required five successive PCR reactions, using plasmid pLJC400 as template. The first reaction was performed using 1.25 units of *Pfu* DNA polymerase in the presence of 2% DMSO. The other four reactions were performed using the Clontech Advantage-GC cDNA PCR kit.

Construction of Plasmid pLJC400ΔClaI. Plasmid pLJC400 was digested with *Cla*I and then treated with T4 DNA ligase at low DNA concentration to favor self-ligation of a 6174 bp fragment. The resulting plasmid, pLJC400ΔClaI, contains the 3′ end of the serine hydroxymethyltransferase gene, the genes for the β and δ cTSOX subunits, and the 5′ end of the gene for the α cTSOX subunit.

Construction of Plasmid pLJC305ΔBsmI. Plasmid pLJC305 was digested with BsmI. The fragment containing vector DNA plus the 3′ end of the gene for serine hydroxymethyltransferase, the entire gene for the β subunit of cTSOX, and the 5′ end of the gene for the δ subunit of cTSOX was purified by agarose gel electrophoresis and submitted to ligation at low concentration to favor self-ligation. Plasmid pLJC305ΔBsmI, obtained after transformation of XL-I Blue cells, contains only a single complete corynebacterial gene, coding for the β subunit of cTSOX.

Construction of Plasmid pLJC500. Plasmid pBluescript II SK(+)ΔKpnI was digested with *Cla*I, treated with the Klenow fragment in the presence of dNTPs for 30 min at 30 °C, and then treated with T4 DNA ligase at low concentration to favor self-ligation. Plasmid pBluescript II SK(+)ΔKpnIΔClaI was obtained after transformation of XL-1 Blue cells; the deletion of the *Cla*I site was confirmed by restriction map analysis. The larger *Xba*I−*Hin*dIII fragment obtained upon digestion of pLJC305 contains the corynebacterial DNA insert. This fragment was subcloned between the *Xba*I and *Hin*dIII sites of pBluescript II SK-(+)ΔKpnIΔClaI to yield plasmid pLJC500.

Construction of Plasmid pβG30A. Left- and right-half reaction fragments (created using the primers in Table 1) were combined with primers 10C and βC146S#1 to generate a 602 bp product which was purified, digested by *Eco*RI and *Sal*I, and then subcloned between the *Eco*RI and *Sal*I sites of pLJC305ΔKpnI to yield plasmid pLJC305ΔKpnI-(βG30A). The latter was digested with *Kpn*I and *Xba*I and the 1862 bp *Kpn*I−*Xba*I fragment was subcloned between the *Kpn*I and *Xba*I sites of pLJC400, to yield plasmid pβG30A.

Construction of Plasmid pβC146S. Left- and right-half reaction fragments (created using the primers in Table 1) were combined with primers βG30A#2 and *Pst*I end to generate the secondary product which was purified, digested with *Sal*I and *Pst*I, and then subcloned between the *Sal*I and *Pst*I sites of pLJC305ΔKpnI to yield plasmid pLJC305ΔKpnI-(βC146S). The latter was digested with *Kpn*I and *Xba*I, and the desired *Kpn*I−*Xba*I fragment was subcloned between the *Kpn*I and *Xba*I sites of pLJC400, to yield plasmid pβC146S.

Construction of Plasmid pβC195S. Left- and right-half reaction fragments (created using the primers in Table 1) were combined with primers *Sal*I end and *Pst*I end to generate a final 352 bp product which was purified, digested with *Sal*I and *Pst*I, and then subcloned between the *Sal*I and *Pst*I sites of pLJC305ΔKpnI to yield plasmid pLJC305ΔKpnI-(βC195S). The latter was digested with *Kpn*I and *Xba*I, and

Table 1: PCR Primers Used To Generate Mutations by the Overlap Extension Method[a]

	left-half primary reaction		right-half primary reaction	
mutation	name	sequence	name	sequence
β(Gly30Ala)	10C	5′-GAGGCTTTTGCCGAG-3′	βG30A#2	5′-CGGCGGCGcCGGCCATGG-3′
	βG30A#1	5′-CCATGGCCGgCGCCGCCG-3′	βC146S#1	5′-GATGATCGGGGAGACTTCCTTG-3′
β(Cys146Ser)	βG30A#2	5′-CGGCGGCGCCGGCCATGG-3′	βC146S#2	5′-CAAGGAAGTCTcCCCGATCATC-3′
	βC146S#1	5′-GATGATCGGGgAGACTTCCTTG-3′	*Pst*I end	5′-GCTCGGAGACCAGGGCC-3′
β(Cys195Ser)	*Sal*I end	5′-GCGCCGCGTGGAGGCC-3′	βC195S#2	5′-CATCCAGAACTcCGAAGTCACC-3′
	βC195S#1	5′-GGTGACTTCGgAGTTCTGGATG-3′	*Pst*I end	5′-GCTCGGAGACCAGGGCC-3′
β(Cys315Ala)	*Pst*I end #2	5′-CCCATCCAGTCCCACCCG-3′	βC351A#2	5′-CTCTACGTCAAtgcCGGCTGGG-3′
	βC351A#1	5′-CCCAGCCGgcaTTGACGTAGAG-3′	*Eco*RI end 2154	5′-GCCACATGGGCCTGGCC-3′
β(His173Ala)	*Sal*I end	5′-GCGCCGCGTGGAGGCC-3′	*Pst*I end	5′-GCTCGGAGACCAGGGCC-3′
	βH173A#1	5′-CCACGTGGTCGgcCTTGGCGATGC-3′	βH173A#2	5′-GCATCGCCAAGgcCGACCACGTGG-3′
β(His173Asn)	*Sal*I end	5′-GCGCCGCGTGGAGGCC-3′	*Pst*I end	5′-GCTCGGAGACCAGGGCC-3′
	βH173N#1	5′-ACGTGGTCGTtCTTGGCGATG-3′	βH173N#2	5′-CATCGCCAAGaACGACCACGT-3′

[a] Mutagenic sites in primers are indicated by lowercase characters.

the 1862 bp *Kpn*I−*Xba*I fragment was subcloned between the *Kpn*I and *Xba*I sites of pLJC400, to yield plasmid pβC195S.

Construction of Plasmid pβC351A. Left- and right-half reaction fragments (created using the primers in Table 1) were combined with primers *Pst*I end #2 and *Eco*RI end 2154 to generate a final 583 bp product which was purified, digested with *Pst*I and *Kpn*I, and subcloned between the *Pst*I and *Kpn*I sites of pLJC305ΔKpnI, to yield plasmid pLJC305ΔKpnI(βC351A). The latter was digested with *Kpn*I and *Xba*I, and the 1862 bp *Kpn*I−*Xba*I fragment was subcloned between the *Kpn*I and *Xba*I sites of pLJC400 to yield plasmid pβC351A.

Construction of Plasmids pβH173A and pβH173N. The left-half primary reaction was conducted using the primer *Sal*I end and mutagenic primer βH173A#1 or βH173N#1. The right-half primary reaction was conducted using the primer *Pst*I end and mutagenic primer βH173A#2 or βH173N#2 (see Table 1 for primer sequences). The two fragments were combined with primers *Sal*I end and *Pst*I end to generate a final 401 bp product containing either the β(His173Ala) or β(His173Asn) mutation. Each PCR product was purified, digested with *Sal*I and *Pst*I, and subcloned between the *Sal*I and *Pst*I sites of pLJC305ΔKpnI to yield the corresponding new plasmids, pLJC305ΔKpnI(βH173A) and pLJC305ΔKpnI(βH173N). The new plasmids were digested with *Kpn*I and *Xba*I. The 1862 bp *Kpn*I−*Xba*I fragment from each digest was subcloned between the *Kpn*I and *Xba*I sites of pLJC400 to yield the final expression plasmids (pβH173A and pβH173N).

Construction of Plasmids pαG139A and pαG139V. For each mutation, a succession of five PCR reactions was performed to create the desired mutation and also eliminate a *Cla*I restriction site via a conservative mutation (see Figure 2 for PCR strategy and Table 2 for primer sequences). Primers *Bam*HI end 2394 and αG139A#5 or αG139V#2 were used to generate the first PCR product, P1 (447 bp). Primers αG139A#4 or αG139V#1 and α*Cla*I#2 were used to generate the second PCR product, P2 (167 bp). Primers α*Cla*I#1 and *Cla*I end 3280 were used to generate the third PCR product, P3 (425 bp). PCR products P1 and P2 were combined with primers *Bam*HI end 2394 and α*Cla*I#2 to generate the fourth PCR product, P4 (596 bp). PCR products P3 and P4 were combined along with primers *Bam*HI end 2394 and *Cla*I end 3280 to generate the final PCR product (998 bp) containing the β(Gly139Ala) or β(Gly139Val) mutation [P5(αG139A) and P5(αG139V), respectively]. These PCR products were purified, digested with *Bam*HI and *Cla*I, and subcloned between the *Bam*HI and *Cla*I sites of pLJC400ΔClaI to yield plasmids pLJC400ΔClaI(αG139A) and pLJC400ΔClaI(αG139V), respectively. The new plasmids were digested with *Xba*I and *Cla*I; the 3264 bp *Xba*I−*Cla*I fragments of interest were each subcloned between the *Xba*I and *Cla*I sites of pLJC500 to yield plasmids pαG139A and pαG139V, respectively.

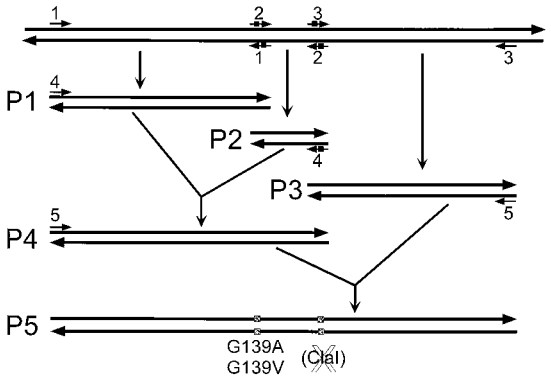

FIGURE 2: The five successive PCR reactions designed to mutate α(Gly139) to Ala or Val and also eliminate a nearby *Cla*I site. The latter corresponds to the *Cla*I site in pLJC400ΔClaI, pLJC400, and pLCJ500 that is not cut by *Cla*I (see Figure 1). Template DNA and PCR products are represented by large pairs of arrows. Primers are shown as short single arrows and are numbered to match the resulting PCR product; a solid square on the arrow tail indicates a mutagenic primer. The first three PCR products (P1, P2, P3) were generated using pLJC400 as template and the indicated primers. PCR product P4 was generated using products P1, P2, and the indicated primers. PCR product P5 was generated using products P3, P4, and the indicated primers.

Table 2: PCR Primers Used To Generate the α(Gly139Ala) and α(Gly139Val) Mutations[a]

name	sequence
*Bam*HI end 2394	5′-GAACTGAACACCCAGGGAG-3′
αG139A#5	5′-CAGGGgCGGCGCCTACCA-3′
αG139V#2	5′-CAGGGaCGGCGCCTACCA-3′
αG139A#4	5′-TGGTAGGCGCCGcCCCTG-3′
αG139V#1	5′-TGGTAGGCGCCGtCCCTG-3′
α*Cla*I#2	5′-GACGGTCGCATCtATCCACGCTG-3′
α*Cla*I#1	5′-CAGCGTGGATaGATGCGACCGTC-3′
*Cla*I end 3280	5′-CGCGGCGGACACCGTGGTGCG-3′

[a] Mutagenic sites in primers are indicated by lowercase characters.

Subcloning the Gene for the β Subunit of cTSOX (soxB) into pET17b. *Nde*I and *Hin*dIII sites were introduced at the 5′ and 3′ ends, respectively, of *soxB* by PCR using the primers *β*start (5′-GAGAATAcatATGGCTGATTTGCT-3′) and *β*end (5′-CAATaAGCtTCATGGTGGCTGCTC-3′). [The lowercase characters indicate the mutations introduced to create the restriction sites (underlined).] The reaction was conducted using 1.25 units of *Pfu* DNA polymerase with pLJC400 as template. The 1252 bp PCR product was digested with *Nde*I and *Hin*dIII, purified, and subcloned between the *Nde*I and *Hin*dIII sites of plasmid pET17b. Plasmid pET-*β* was obtained after transformation of XL-1 Blue cells, and the sequence of the insert was verified. For expression studies, pET-*β* was transferred into BL21(DE3) cells.

Subcloning the Gene for the α Subunit of cTSOX (soxA) into pET23a. PCR was used to introduce *Nde*I and *Xho*I sites at the 5′ and 3′ ends of *soxA*, respectively. The reaction was conducted using the primers αstart (5′-GGAGGATCCatATGAGCCAGAACACG-3′) and αend (5′-atGTGcTcgagGCCATCGCGGCGGCTC-3′), the Clontech Advantage-GC cDNA PCR kit, and plasmid pLJC 400 as template. (The silent mutations in the first two bases at the 5′ end of primer αend were introduced to reduce the high GC content.) The introduction of the *Xho*I site eliminates the stop codon and inserts codons for leucine and glutamate at the 3′ end of the soxA gene. The PCR product (2923 bp) was digested with *Nde*I and *Xho*I, purified, and subcloned between *Nde*I and *Xho*I sites of plasmid pET23a, a vector designed to incorporate a $(His)_6$ tag at the C-terminus of the recombinant protein. After transformation of XL-1 Blue cells, plasmids from several colonies were purified, sequenced, and found to contain between one and three mutations within the 3 kb *soxA* gene. Using unique restriction sites, a final mutation-free construct (plasmid pET-α) was generated by replacing mutation-containing sections in one plasmid with the corresponding error-free section from another plasmid. When BL21(DE3) cells were transformed with plasmid pET-α, expression of the α subunit was observed but expression levels were found to vary greatly in different experiments, prompting a search for a different expression system.

Subcloning of the cTSOX soxA Gene from a pET to a pBluescript Derivative. Plasmid pET-α was digested with *Nde*I and *Xho*I. The resulting 2903 bp *Nde*I−*Xho*I fragment containing the *soxA* gene [without the C-terminal $(His)_6$ tag] was subcloned between the *Nde*I and *Xho*I sites of plasmid pME430 to yield plasmid p-ALPHA-1. (Plasmid pME430 is a pBluescript derivative similar to pLJC400; it contains a unique *Nde*I site at the 3′ end of the gene coding for SHMT and a unique *Xho*I site in the vector multicloning region downstream of the TSOX genes.[2]) To reintroduce a C-terminal $(His)_6$ tag, a region in plasmid pET-α that included the 3′ end of the *soxA* gene, the $(His)_6$ tag, and downstream vector sequence was amplified in a PCR reaction using *Pfu* polymerase and primers *Xho*I end (5′-GAGCCGCCGCGATGGCCTCG-3′) and *Kpn*I end #1 (5′-ggggtaCCGGATATAGTTCCTC-3′). [The lowercase characters indicate mutations introduced to create a *Kpn*I restriction site (underlined).] The 183 bp PCR product was digested with *Xho*I and *Kpn*I. The 155 bp *Xho*I−*Kpn*I fragment was subcloned between the *Xho*I and the *Kpn*I sites at the 3′ end of *soxA* in pALPHA-1 to yield plasmid pALPHA-2. XL-1 Blue cells were transformed with plasmid pALPHA-2 for expression studies.

Enzyme Expression and Purification. Cells expressing recombinant, wild-type cTSOX (XL-1 Blue/pLJC400) were grown in LB (*18*) containing ampicillin or carbenicillin (100 μg/mL) at 29 °C, as previously described (*10*). The same conditions and host cell were used for expression of the following mutants: *β*(Cys141Ser), *β*(Cys195Ser), *β*-(Cys351Ala), and *β*(His173Asn). The α(Gly149Ala) mutant was isolated from XL-1Blue/pαG139A cells grown in the same medium (initially at 29 °C) but harvested 3 days after induction at 15 °C. The α subunit was isolated from XL-1 Blue cells/pALPHA-2 cells grown in the same medium; the growth temperature was switched from 29 to 25 °C prior to induction. For the expression of other mutants or subunits, transformed XL-1 Blue or BL21(DE3) cells were grown in LB or tryptone−phosphate (*19*) containing ampicillin or carbenicillin (100 μg/mL) at various temperatures, as indicated in the Results section. Cells were harvested and cell lysates prepared as described by Chlumsky et al. (*10*).

The natural form of cTSOX was isolated from *Corynebacterium* sp. P-1 as previously described (*10*). Unless otherwise indicated, recombinant cTSOX (wild-type and mutant forms) were purified from cell lysates using a procedure similar to that previously described (*10*). The *β*-(His173Asn) cTSOX mutant bound more tightly to the phenyl-Sepharose column than wild-type enzyme and was not eluted with the standard gradient (0.4−0.0 M ammonium sulfate in 50 mM potassium phosphate buffer, pH 7.0, containing 5.0 mM EDTA) but did elute with deionized water. Lysate from cells expressing the α subunit by itself was dialyzed against 50 mM sodium phosphate buffer, pH 7.0, containing 500 mM NaCl and 20% glycerol. The dialyzed sample was mixed with a cobalt affinity matrix (Talon affinity resin). The matrix was washed twice with dialysis buffer in a batchwise procedure. The washed matrix was mixed with dialysis buffer containing 15 mM imidazole, and the suspension was poured into a glass column. Fractions were collected as the matrix settled to form a 1.5 × 4.5 cm column. The column was then washed with dialysis buffer containing 150 mM imidazole. Fractions were pooled as detailed in Results, concentrated (Amicon YM-10), and dialyzed against dialysis buffer to remove imidazole. The cloning, expression, and isolation of the recombinant form of TSOX from *P. maltophilia* (pTSOX) and the purification of the natural enzyme will be published elsewhere.

Protein concentration was determined by the Bradford method (*20*) or from the absorbance at 280 nm using the extinction coefficient ($E^{1\%} = 13.1$) as reported by Suzuki (*21*), unless otherwise indicated. Enzyme activity was measured using the discontinuous Nash assay (*22*, *23*), the NADH coupled assay (*10*, *24*), or the horseradish peroxidase coupled assay. The latter assay was conducted in 50 mM potassium phosphate buffer, pH 8.0, containing 120 mM sarcosine, under conditions otherwise identical to those previously described (*12*).

Gel Electrophoresis. Electrophoresis was conducted as previously described (*10*) except that 7% and 12% resolving gels were used for native and SDS−PAGE, respectively. Proteins were detected by staining with Coomassie blue (*25*).

[2] M. Eschenbrenner and M. S. Jorns, unpublished results,

TSOX activity was visualized as a pink band using iodonitrotetrazolium violet as a redox indicator dye, as previously described (*24*). As will be described, purification of the β-(His173Asn) cTSOX mutant in the absence of stabilizing agents yields a preparation containing only α and γ subunits. To determine the molar ratio of these subunits, the SDS−PAGE gel was scanned (Bio-Rad imaging densitometer, model GS-670) and analyzed using the Molecular Analyst program (Bio-Rad). The volume (area × absorbance) of each band was estimated for samples of mutant or wild-type enzyme run on the same gel using the volume report function. The relative volumes measured for the α and γ bands in wild-type cTSOX were used as a standard for a 1:1 complex.

Antibody Preparation. Rabbit antibodies against a pure sample of recombinant cTSOX were prepared by HTI Bio-Products, Inc., using a standard protocol. Briefly, booster shots were given 21, 35, and 49 days after the initial injection. The rabbits were bled at 46, 59, and 66 days after the initial injection. Serum was isolated from each bleed and tested for the presence of the cTSOX antibodies using an ELISA assay. The highest titer of antibodies was observed for the last bleed which was used for all studies.

Western Blot Analysis. Samples (15 μg of protein per lane) were subjected to native or SDS−PAGE as described above. The gel (20 cm × 20 cm) and sheets of Whatman 3MM paper (precut to the gel dimensions) were equilibrated for 5 min with transfer buffer (20% methanol, 20 mM Tris, 150 mM glycine, pH 8.3). Nitrocellulose membranes (Bio-Rad) (precut to the gel dimensions) were wet with deionized water for 5 min. The transfer "sandwich" (three sheets of paper, acrylamide gel, nitrocelluose membrane, three sheets of paper) was assembled in a transfer cassette and placed into the tank of a Bio-Rad Trans-Blot cell filled with transfer buffer. The transfer was conducted at 4 °C (20 V, 16 h); all subsequent steps were performed at room temperature. After transfer, the nitrocellulose membrane was removed and washed three times for 20 min each with MTTBS. MTTBS was prepared by adding 2 tsp of powdered milk to 1 L of TTBS [8 g/L NaCl, 0.2 g/L KCl, 3 g/L Tris-HCl, pH 7.4, 0.2% (v/v) Tween 20]. The primary antibody against cTSOX was diluted 10 000-fold with TTBS and added to a pouch containing the nitrocellulose membrane. The pouch was sealed and rocked for 90 min, and the membrane was then washed four times for 10 min each with MTTBS. A secondary antibody [mouse peroxidase conjugated monoclonal anti-rabbit IgG (γ-chain specific) antibody] (Sigma) was diluted 5000-fold with TTBS and added to a pouch containing the nitrocellulose membrane. After being rocked for 90 min, the membrane was washed two times for 15 min each with MTTBS and two times for 15 min each with TTBS. The membrane was then incubated with freshly prepared developing solution [1 tablet of 3,3′-diaminobenzidine (DAB) (Sigma) and 1 tablet of urea−H_2O_2 (Sigma) per 5 mL of deionized water] for 1−3 min when color development was stopped by washing the membrane with deionized water. Membranes were air-dried.

Spectroscopy. Absorption spectra were recorded at 25 °C using a Perkin-Elmer Lambda 3B spectrophotometer, unless otherwise indicated. To determine the amount of covalently bound FMN and noncovalent FAD, samples of TSOX in 10 mM potassium phosphate buffer, pH 8.0, containing 0.3 mM EDTA were diluted with an equal volume of 6 M guanidine hydrochloride at 25 °C. The sample was microfiltered (Microcon-30), and the absorbance of the filtrate at 450 nm was used to estimate the contribution due to noncovalently bound FAD (ϵ_{450} = 11.5 mM^{-1} cm^{-1}). The absorbance of the unfiltered solution at 450 nm was corrected for the contribution due to FAD, and the amount of covalently bound FMN was estimated using an extinction coefficient for free FMN (ϵ_{450} = 12.1 mM^{-1} cm^{-1}). Protein concentration was estimated using an extinction coefficient at 280 nm determined on the basis of amino acid composition (ϵ_{280} = 216.2 mM^{-1} cm^{-1} for wild-type cTSOX; ϵ_{280} = 130.6 mM^{-1} cm^{-1} for a 1:1 $\alpha\gamma$ complex; ϵ_{280} = 106.5 mM^{-1} for the α subunit), after correcting the observed absorbance of the unfiltered solution at 280 nm (when necessary) for the contribution due to FMN (ϵ_{280} = 20.6 mM^{-1} cm^{-1}), FAD (ϵ_{280} = 22.3 mM^{-1} cm^{-1}), and NAD^+ (ϵ_{280} = 3.5 mM^{-1} cm^{-1}). Extinction coefficients for free FMN, FAD, and NAD^+ were measured in 3 M guanidine hydrochloride. To determine NAD^+ content, a separate enzyme sample was precipitated with 10% TCA. The protein pellet was redissolved in 6 M guanidine hydrochloride, and protein was determined on the basis of the absorbance at 280 nm, after correcting for the contribution due to covalently bound FMN (when present). TCA was removed from the supernatant by extraction seven times with an equal volume of ether. Residual ether was removed by bubbling argon through the solution. The TCA-free supernatant was diluted 1:1 with 100 mM sodium pyrophosphate buffer, pH 8.8, containing 45 mM semicarbazide, and then 128 mM ethanol was added. The NAD^+ content was determined on the basis of the amount of NADH formed after a 6 min incubation at 25 °C with yeast alcohol dehydrogenase (2.6 units/mL). NADH formation was estimated on the basis of the increase in absorbance at 340 nm (ϵ_{340} = 6.2 mM^{-1} cm^{-1}). Spectra obtained during titration of pTSOX with sulfite or methylthioacetate were corrected for dilution.

RESULTS

Is the Reactive Cysteine in the β Subunit? About half of the covalent FMN in recombinant cTSOX forms a reversible 4a-adduct with an unidentified cysteine residue. The adduct is not found in the natural enzyme. Pure preparations of recombinant enzyme exhibit larger values for the ratio A_{280}/A_{450} than the natural enzyme because the adduct exhibits negligible absorbance at 450 nm (Table 3, Scheme 2). Preparations of cTSOX that contain the 4a-adduct also exhibit increased values for the ratio A_{368}/A_{450} (Table 3) and a lag in coupled catalytic assays.

The 8α-position of FMN is attached to the β subunit. To determine whether this subunit also contained the reactive cysteine, the three cysteine residues in the β subunit in cTSOX were changed to serine or alanine. Good expression was observed for the Cys → Ser mutation at β(Cys141) or β(Cys195) but not β(Cys351). Good expression was observed for the β(Cys351Ala) mutant. The purified mutant enzymes exhibited specific activity values similar to those of the wild-type recombinant cTSOX or the natural enzyme isolated from *Corynebacterium* sp. P-1 (Table 3). All of the mutant enzymes and wild-type recombinant cTSOX exhibited a pronounced lag in an NADH peroxidase coupled assay and elevated values for the spectral ratios A_{280}/A_{450} and A_{368}/A_{450} as compared with the natural enzyme. The lags and differ-

Table 3: Comparison of Natural TSOX from *Corynebacterium* sp. P-1 with Wild-Type and Mutant Recombinant Enzymes

enzyme preparation	specific activity (units/mg)[a]	spectral properties: untreated A_{280}/A_{450}	untreated A_{368}/A_{450}	MMTS treated[b] A_{280}/A_{450}	MMTS treated[b] A_{368}/A_{450}	4a-thiolate adduct (%)[d]
natural	9.0	11.6	0.83	(11.6)[c]	(0.83)[c]	0
recombinant						
wild type	9.9	15.4	0.95	11.4	0.86	49 (52)
β(Cys141Ser)	6.3	18.0	1.1	13.3	0.80	71 (52)
β(Cys195Ser)	8.9	18.4	1.0	14.4	0.87	74 (44)
β(Cys351Ala)	10	16.2	1.1	14.4	0.91	57 (22)

[a] Enzyme activity was estimated by measuring formaldehyde production using the discontinuous Nash assay (*22*, *23*). [b] Samples were reacted with 1.0 mM MMTS in 10 mM potassium phosphate buffer, pH 8.0 at 25 °C, as previously described (*10*). [c] The spectral properties of the natural enzyme are not affected by MMTS (*10*). [d] Estimated by comparing A_{280}/A_{450} of the untreated recombinant enzyme with the natural enzyme. Values shown in parentheses were estimated by comparing A_{280}/A_{450} of the untreated recombinant enzyme with the corresponding MMTS-treated preparation.

Table 4: Comparison of Natural TSOX from *P. maltophilia* with the Recombinant Enzyme

enzyme preparation	spectral properties: untreated A_{280}/A_{450}	untreated A_{368}/A_{450}	H_2O_2 treated[a] A_{280}/A_{450}	H_2O_2 treated[a] A_{368}/A_{450}	4a-thiolate adduct (%)[c]
natural	13.9	0.92	(13.9)[b]	(0.92)[b]	0
recombinant[d]					
lac promoter	19.2	1.06	13.3	0.84	61
T7 promoter	16.4	0.98	13.3	0.84	38

[a] Samples in 10 mM potassium phosphate buffer, pH 8.0 at 25 °C, were reacted with successive aliquots of 20 mM H_2O_2 until no further increase in absorbance at 450 nm was observed. The larger amount of H_2O_2 required, as compared with recombinant cTSOX (2 mM) (*10*), is due to a catalase contaminant in the recombinant pTSOX preparation. [b] The spectral properties of the natural enzyme are not affected by H_2O_2. [c] Estimated by comparing A_{280}/A_{450} of the untreated recombinant enzyme with the value observed after reaction with H_2O_2. [d] Recombinant pTSOX was expressed in two different *E. coli* host strains under the control of different promoters, as described in the text.

ences in spectral ratios were largely eliminated by treatment with MMTS (Table 3). In each case, the changes induced by MMTS were reversed upon treatment with DTT and dialysis, as previously reported for the wild-type recombinant enzyme (*10*).

The amount of 4a-thiolate adduct in untreated wild-type recombinant cTSOX (49%) or the mutant enzymes (57−74%) was estimated by comparison of the spectral ratio A_{280}/A_{450} with that observed for the natural enzyme. Somewhat lower values for the mutant enzymes were estimated by comparison of the ratio A_{280}/A_{450} observed for untreated versus MMTS-treated enzyme (Table 3). In either case, it is clear that all mutant enzymes contain a significant amount of 4a-thiolate adduct. The results show that none of the cysteine residues in the β subunit is involved in the formation of the 4a-adduct or is important for catalysis.

Is a 4a-Thiolate Adduct Found in Recombinant TSOX from Other Sources? TSOX from *Arthrobacter* sp. 1-IN (aTSOX) exhibits the same subunit and coenzyme composition and shares 96% amino acid sequence identity with cTSOX (*26*). A recent study, however, failed to detect a 4a-adduct in recombinant aTSOX. We recently cloned and expressed TSOX from *P. maltophilia* (pTSOX). pTSOX is less similar to cTSOX than is aTSOX, as judged by the amino acid sequence identity observed with pTSOX and cTSOX (α, 84%; β, 96%; γ, 72%; δ, 80%).[2]

A 4a-adduct is not found in the natural form of pTSOX isolated from *P. maltophilia*,[3] similar to that observed with cTSOX. Recombinant pTSOX, however, exhibits a lag in a horseradish peroxidase coupled assay and increased values for the spectral ratios A_{280}/A_{450} and A_{368}/A_{450} as compared with the natural enzyme (Table 4). The 4a-adduct in recombinant pTSOX is disrupted by reaction with H_2O_2, as judged by characteristic changes in the visible absorption spectrum of the enzyme (Figure 3). H_2O_2 treatment also eliminates the lag in the coupled assay and shifts the spectral ratios to values similar to those of the natural enzyme isolated from *P. maltophilia* (Table 4).

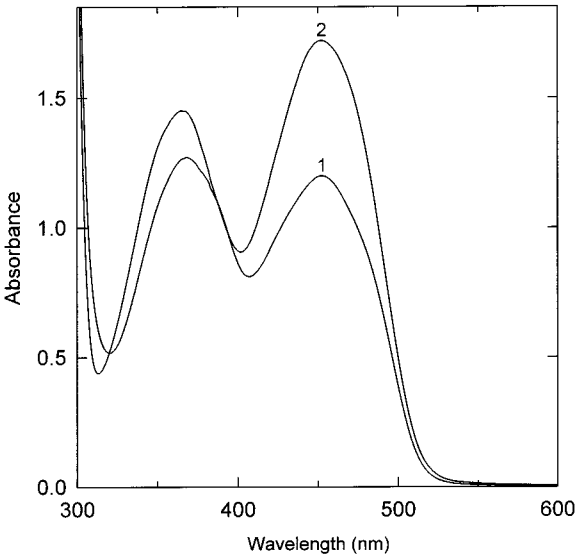

FIGURE 3: Reaction of recombinant pTSOX with hydrogen peroxide. Curve 1 is the absorption spectrum of the untreated enzyme in 10 mM potassium phosphate buffer, pH 8.0, at 25 °C. Curve 2 was recorded after reaction with hydrogen peroxide, as detailed in the legend to Table 4.

The recombinant forms of cTSOX and pTSOX are typically isolated in our laboratory from transformed *E. coli* XL-1 Blue cells where the enzymes are expressed under the

[3] G. Zhao and M. S. Jorns, unpublished results.

control of the *lac* promoter, using pBluescript II SK(+) as vector. The recombinant form of aTSOX was expressed under the control of the T7 promoter using a pET vector with *E. coli* BL21(DE3) as host cell (*26*). We therefore investigated the effect of a similar expression system on the 4a-adduct content of pTSOX. In fact, a substantial amount of 4a-adduct (38%) was found in preparations of pTSOX when expression of the recombinant enzyme was placed under the control of the T7 promoter using a pET vector (pET17b) and *E. coli* BL21(DE3) as host cell (Table 4).

Role of the Covalent Flavin Link: Mutation of β(His173) to Ala. Studies to evaluate the role of the covalent link between the 8α-position of FMN and the β subunit of cTSOX were initiated by mutating β(His173) to alanine. Wild-type recombinant cTSOX constitutes about 30% of the protein in cell lysates (*10*) which exhibit a prominent band on native gels (Figure 4A, lane 1), comigrating with pure enzyme (Figure 4A, lane 6). Expression of the β(His173Ala) mutant was not detected when cell lysates were subjected to native gel electrophoresis (Figure 4A, lane 3) or assayed for TSOX activity. SDS−PAGE analysis readily detects the α subunit in wild-type lysates (Figure 4C, lane 1). All four subunits are detected when wild-type lysates are subjected to Western blot analysis using a polyclonal antibody (Figure 4D, lane 1). No subunits were detected when mutant lysates were subjected to SDS−PAGE (Figure 4C, lane 3) or Western blot analysis (Figure 4D, lane 3). Inclusion body formation could be ruled out since no subunits were detected when mutant cell pellets were subjected to SDS−PAGE analysis (data not shown). The results show that the β(His173Ala) mutation blocks protein expression in cells grown under standard conditions (LB, 29 °C).[4]

Growth of cells on an enriched medium (tryptone−phosphate) at reduced temperature can overcome difficulties in the expression of recombinant proteins (*19*). Indeed, mutant lysates from cells grown on tryptone−phosphate medium at 25 °C exhibited subunit expression levels similar to those of the wild-type enzyme, as judged by SDS−PAGE (Figure 4C, lane 5) or Western blot (Figure 4D, lane 5) analysis. No subunits were detected in control lysates (lane 4 in Figure 4C,D). Despite the enormous effect on subunit expression, the new growth conditions did not resolve the subunit assembly problem, as judged by native gel analysis of cell lysates where the mutant protein was barely detectable (Figure 4A, lane 5). When the native gel was subjected to Western blot analysis, a thin, weak band was seen with the mutant lysate (Figure 4B, lane 5) that appeared to comigrate with the pure, wild-type enzyme (Figure 4B, lane 6). However, the mutant lysate also exhibited a larger, diffuse, slower migrating band that may reflect the presence of a heterogeneous mixture of oligomeric forms. The latter might account for the absence, in native gels stained for protein, of a prominent band, comigrating with the wild-type enzyme. Attempts to overcome the subunit assembly problem by growing cells at lower temperature (15 °C) or by adding riboflavin (20−200 μM) to the tryptone−phosphate growth medium were unsuccessful.

Role of the Covalent Flavin Link: Mutation of β(His173) to Asn. Previous studies suggest that alanine is not always a benign, neutral replacement for histidine. Asparagine can be a much better substitute in certain locations, possibly reflecting a requirement for a degree of steric bulk that cannot be satisfied by alanine (*27*). Indeed, the β(His173Asn) mutant of cTSOX was found to exhibit apparently normal subunit expression and assembly even when grown under standard conditions (LB, 29 °C), as judged by native gel electrophoresis. A distinct protein band is observed with the mutant lysate (Figure 5, lane 4) that comigrates with wild-type cTSOX (Figure 5, lanes 3 and 6). The β(His173Asn) mutant is, however, catalytically inactive and does not exhibit a band when the native gel is stained for activity (Figure 5, lane 9),

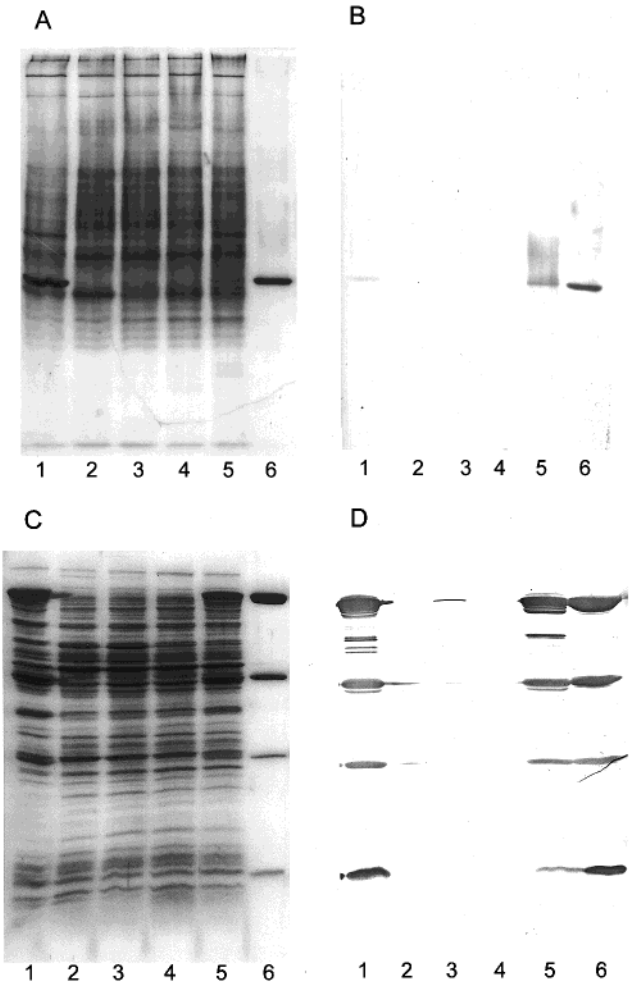

FIGURE 4: Expression of the β(His173Ala) mutant of cTSOX. Panel A is a native gel stained for protein, and panel B is the corresponding Western blot developed using a polyclonal antibody against wild-type recombinant cTSOX. Panel C is an SDS gel stained for protein, and panel D is the corresponding Western blot. In each of the four panels, an aliquot of a given protein sample was run in lanes labeled with the same number. Cells were grown on LB medium at 29 °C or tryptone−phosphate (TP) at 25 °C, as indicated. Lanes 1 and 6 (LB, 29 °C) are lysate and purified enzyme, respectively, from cells (XL-1 Blue/pLJC400) expressing wild-type recombinant cTSOX; lanes 2 (LB, 29 °C) and 4 (TP, 25 °C) are lysates from control cells containing nonrecombinant vector [XL-1 Blue/pBluescript SK(+)]; lanes 3 (LB, 29 °C) and 5 (TP, 25 °C) are lysates from cells (XL-1 Blue/pβH173A) designed to express the β(His173Ala) cTSOX mutant. A faint band, comigrating with pure cTSOX, was seen on the original, native gel (panel A) with lysate from mutant cells grown on TP at 25 °C (lane 5) but not with the corresponding control extract (lane 4). [The reason for the weak reaction of the polyclonal antibody with the wild-type enzyme in crude extracts (Figure 4B, lane 1) is unclear.]

[4] Expression as an unstable protein that is rapidly degraded cannot be ruled out.

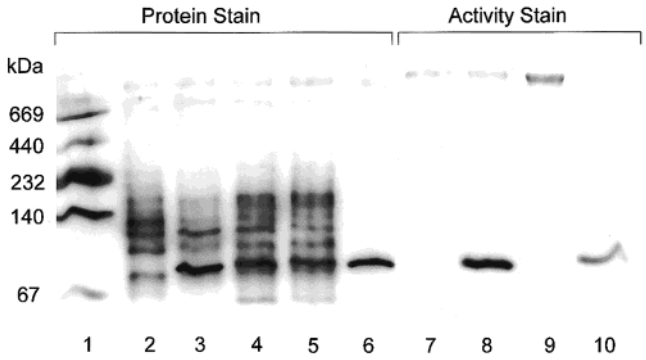

FIGURE 5: Expression of the β(His173Asn) mutant of cTSOX. Lysates were prepared from cells grown on LB medium at 29 °C, unless otherwise indicated. Lanes: 1, molecular mass markers; 2 and 7, lysate from control cells containing nonrecombinant vector [XL-1 Blue/pBluescript SK(+)]; 3 and 8, lysate from cells (XL-1 Blue/pLJC400) expressing wild-type recombinant cTSOX; 4, 5, and 9, lysate from cells (XL-1 Blue/pβH173N) expressing the β-(His173Asn) mutant and grown at 29, 25 (TP), and 25 °C, respectively; 6 and 10, pure wild-type cTSOX.

unlike wild-type enzyme (Figure 5, lanes 8 and 10). Expression of the β(His173Asn) mutant was not enhanced by growth on tryptone−phosphate medium at 25 °C (Figure 5, lane 5), unlike the β(His173Ala) mutant.

The β(His173Asn) mutant was purified using the four-step procedure developed for the wild-type enzyme: ammonium sulfate fractionation and gel filtration, followed by chromatography on phenyl-Sepharose and DEAE-Sephacel (*10*). Isolation of the catalytically inactive mutant was monitored by Western blot (Figure 6A) or SDS−PAGE (Figure 6B) analysis. All four subunits are present in the cell lysate (Figure 6A, lane 3) and retained up to and including the gel filtration step (Figure 6A, lane 4). Purification is, however, accompanied by a progressive loss of the β subunit, which is particularly pronounced after the phenyl-Sepharose step (Figure 6A, lane 5; Figure 6B, lane 1). The loss of the β subunit appears to coincide with the accumulation of unidentified bands that react with the polyclonal antibody and migrate at an intermediate rate as compared with the α and β subunits. This material is diminished but not entirely eliminated by the DEAE-Sephacel step (Figure 6A, lane 6). Depletion of the δ subunit is first evident in the eluate from the phenyl-Sepharose column (Figure 6A, lane 5; Figure 6B, lane 1) and complete after the DEAE-Sephacel step. The final preparation contains only two subunits, α and γ, as judged by Western blot (Figure 6A, lane 6) or SDS−PAGE analysis (Figure 6B, lane 5). The results strongly implicate the covalent flavin link as an important structural element in wild-type cTSOX.

Characterization of the $\alpha\gamma$ *Complex*. A nearly pure $\alpha\gamma$ complex was isolated upon purification of the β(His173Asn) mutant, as described above. The subunit stoichiometry of this complex was estimated on the basis of the relative amounts of the α and γ subunits detected upon SDS−PAGE analysis of the peak fraction from the DEAE-Sephacel column (Figure 6B, lane 5). Results obtained for the α and γ subunits in pure wild-type cTSOX were used as a standard for a 1:1 complex, as detailed in Experimental Procedures. The analysis indicates that the purified complex contains approximately stoichiometric amounts of the α and γ subunits ($\gamma/\alpha = 0.95 \pm 0.25$).

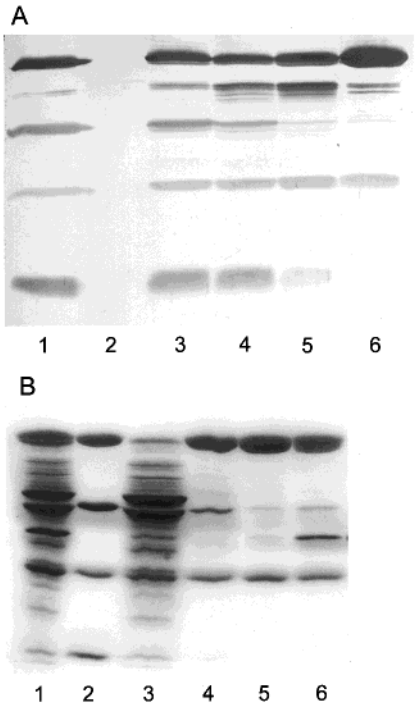

FIGURE 6: Analysis of fractions obtained during the purification of the β(His173Asn) mutant of cTSOX in the absence of stabilizing agents. Panel A shows the Western blot analysis of an SDS gel. Lane 1 is pure wild-type cTSOX. Lane 2 is lysate from control cells containing nonrecombinant vector [XL-1 Blue/pBluescript SK-(+)]. The lysate from cells (XL-1 Blue/pβH173N) expressing the β(His173Asn) cTSOX mutant (lane 3) was purified by ammonium sulfate fractionation (not shown), gel filtration on Ultrogel AcA 34 (lane 4), hydrophobic chromatography on phenyl-Sepharose (lane 5), and anion-exchange chromatography on DEAE-Sephacel (lane 6). Panel B is an SDS gel stained for protein. Lane 1 is the eluate from the phenyl-Sepharose column. Lane 2 is pure wild-type cTSOX. Lane 3 is an initial wash of the DEAE-Sephacel column. Lanes 4−6 are fractions (12, 15, and 18, respectively) eluted when the DEAE-Sephacel column was developed with a salt gradient. Fractions 12, 15, and 18 are the leading edge, peak fraction, and trailing edge of the DEAE-Sephacel column eluate. Fractions 14−16 were pooled for NAD^+ analysis.

The α and β subunits each contain an NH_2-terminal ADP-binding motif that could serve as part of the binding site for FAD or NAD^+ in the wild-type enzyme. The location of the binding sites for these coenzymes was, however, not known. The isolation of a complex ($\alpha\gamma$) that contained the α subunit but not the β subunit provided an opportunity to address this issue. The $\alpha\gamma$ complex did not exhibit significant absorbance in the visible region, ruling out the presence of FAD. To determine whether the complex contained NAD^+, the protein was precipitated with TCA. The supernatant was extracted with ether to remove TCA, diluted with buffer containing semicarbazide (45 mM), and then mixed with ethanol (128 mM). The diluted supernatant exhibited an absorption maximum at 260 nm and a broad, weak shoulder around 300 nm (Figure 7, curve 1). Addition of yeast alcohol dehydrogenase resulted in the appearance of a new absorption band at 340 nm attributed to NADH formation (Figure 7, curve 2). The NAD^+ concentration (42 μM) was estimated on the basis of the increase in absorbance at 340 nm. The corresponding concentration of the $\alpha\gamma$ complex (44 μM) was determined on the basis of the observed absorbance at 280 nm when the pellet of the TCA-precipitated enzyme was redissolved in 6 M guanidine hydrochloride, as detailed in

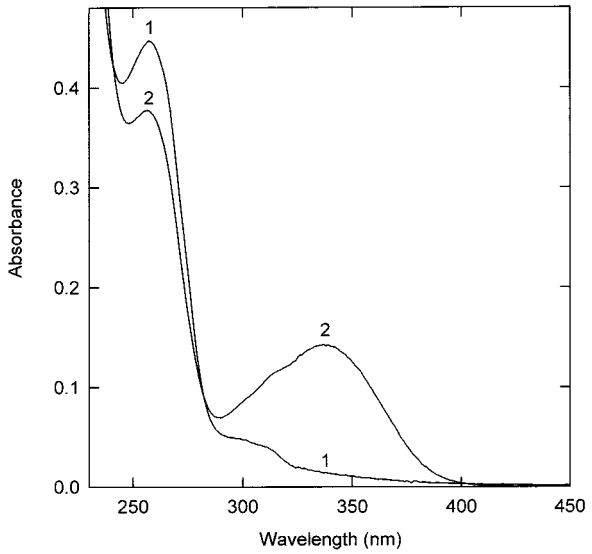

FIGURE 7: NAD^+ content of the $\alpha\gamma$ complex isolated upon purification of the β(His173Asn) mutant of cTSOX in the absence of stabilizing agents. Curve 1 is the absorption spectrum of the supernatant obtained after precipitation of the $\alpha\gamma$ complex with TCA, ether extraction, 1:1 dilution with 100 mM sodium pyrophosphate buffer, pH 8.8, containing 45 mM semicarbazide, and addition of 128 mM ethanol. Curve 2 was recorded 6 min after addition of yeast alcohol dehydrogenase (2.6 units/mL) at 25 °C.

Experimental Procedures. The results show that the $\alpha\gamma$ complex contains a nearly stoichiometric amount of NAD^+ (0.95 mol/mol of complex) and strongly suggest that the NAD^+ binding site is in the α subunit.

Purification of the β(His173Asn) Mutant in the Presence of Stabilizing Agents. Purification of the β(His173Asn) mutant was conducted in the presence of 10% glycerol, 10 μM FAD, and 10 μM FMN in an attempt to prevent loss of the β and δ subunits. Western blot analysis of various fractions during the purification shows that the presence of these stabilizing agents does not prevent loss of the β subunit. As observed in the absence of stabilizing agents, loss of the β subunit is especially pronounced after the phenyl-Sepharose step and accompanied by the appearance of immunoreactive material with a migration rate intermediate between the α and β subunits (Figure 8, lane 6). The presence of the stabilizing agents does, however, prevent loss of the δ subunit. The final preparation contained three subunits, α, γ, and δ (Figure 8, lanes 7 and 8) but no flavin, consistent with the loss of the β subunit and its flavin binding sites.

Expression of the α Subunit by Itself. The $\alpha\gamma$ complex was found to contain 1 mol of NAD^+, implicating the α subunit as the binding site for NAD^+. Direct evidence was sought by expressing the α subunit from cTSOX by itself. The gene encoding the α subunit of cTSOX (*soxA*) was amplified by PCR and subcloned between the *Nde*I and *Xho*I sites of plasmid pME430, a pBluescript derivative. The final expression plasmid was generated after inserting a PCR product at the 3′ end of the *soxA* gene that was designed to incorporate a $(His)_6$ tag at C-terminal end of the protein. Good expression of the His-tagged α subunit was observed when cells were induced at 25 °C. The α subunit was purified using a cobalt affinity column. About one-third of the α subunit applied to the column was eluted by washing with 15 mM imidazole (12.8 mg); the remainder (24.7 mg) was recovered upon washing with 150 mM imidazole. The 150 mM imidazole eluate was combined into two pools (pool A, tubes 30−35; pool B, tubes 36−42.). All three fractions contained highly purified α subunit, as judged by SDS−PAGE or Western blot analysis (Figure 9). None of the fractions exhibited significant absorbance in the visible region

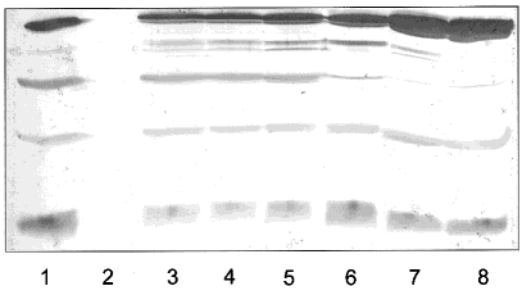

FIGURE 8: Western blot analysis of fractions obtained during the purification of the β(His173Asn) mutant of cTSOX in the presence of stabilizing agents (10% glycerol, 10 μM FAD, and 10 μM FMN). Lane 1 is pure wild-type cTSOX. Lane 2 is lysate from control cells containing nonrecombinant vector [XL-1 Blue/pBluescript SK-(+)]. Lysate from cells (XL-1 Blue/pβH173N) expressing the β-(His173Asn) cTSOX mutant (lane 3) was purified by ammonium sulfate fractionation (lane 4), gel filtration on Ultrogel AcA 34 (lane 5), hydrophobic chromatography on phenyl-Sepharose (lane 6), and anion-exchange chromatography on DEAE-Sephacel (lane 7, side fraction; lane 8, main fraction).

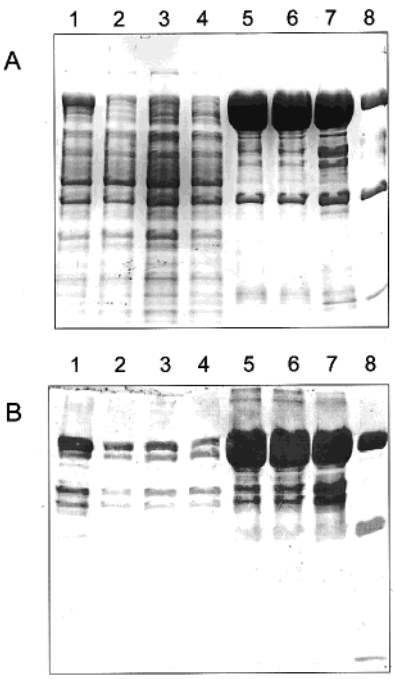

FIGURE 9: Expression of the α subunit from cTSOX by itself. Panel A is an SDS gel stained for protein. Panel B is the corresponding Western blot. In each panel, an aliquot of a given protein sample was run in lanes labeled with the same number. Dialyzed cell lysate (lane 1) was mixed with cobalt affinity matrix. Lanes 2 and 3 are the eluates obtained when the matrix was washed (twice) with dialysis buffer (50 mM sodium phosphate, pH 7.0, containing 500 mM sodium chloride and 20% glycerol). The matrix was then mixed with dialysis buffer containing 15 mM imidazole and poured to form a column. Fractions collected as the column settled were combined into two pools: fractions 1−11 (lane 4) and fractions 12−29 (lane 5). Fractions collected upon washing the column with dialysis buffer containing 150 mM imidazole were combined into two pools: fractions 30−35 (pool A, lane 6) and fractions 36−42 (pool B, lane 7). Pure wild-type cTSOX (lane 8) exhibits bands due to the α, β, and γ subunits but not the δ subunit which ran off the gel.

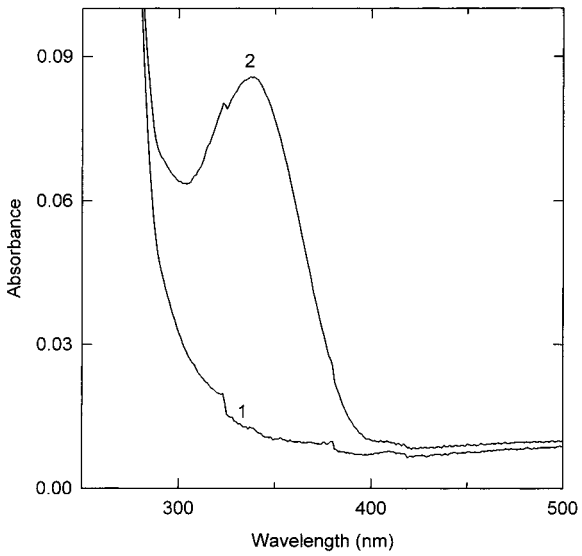

FIGURE 10: NAD^+ content of the α subunit from cTSOX. Curve 1 is the absorption spectrum of the supernatant obtained after TCA precipitation and further treatment as described in the legend to Figure 7. Curve 2 was recorded 6 min after addition of yeast alcohol dehydrogenase (2.6 units/mL) at 25 °C. The experiment shown was conducted with α subunit purified by cobalt affinity chromatography (150 mM imidazole eluate, pool A), as described in the text.

and therefore did not contain flavin. An aliquot of each fraction was denatured with TCA. The NAD^+ content in each of the TCA-free supernatants was estimated after addition of semicarbazide, ethanol, and alcohol dehydrogenase, as described above for the $\alpha\gamma$ complex. NAD^+ was present in all three supernatants, as illustrated by the results obtained with the supernatant from the 150 mM imidazole eluate, pool A (Figure 10). Data analysis showed that each fraction contained a nearly stoichiometric amount of NAD^+: 0.90 mol/mol of α (15 mM imidazole eluate); 1.1 mol/mol of α (150 mM imidazole eluate, pool A); 1.3 mol/mol of α (150 mM imidazole eluate, pool B). The results provide definitive evidence for the presence of the NAD^+-binding site in the α subunit.

Mutation of α(Gly139) to Ala or Val. The ADP-binding motif near the NH_2 terminus of the 967 residue α subunit from cTSOX contains three highly conserved glycine residues (GX**G**^{139}XXG). Studies with other $NAD(P)^+$-binding proteins suggested that a Gly → Ala mutation of the second glycine in this motif would cause a significant decrease in nucleotide binding affinity (*28*, *29*). In an attempt to generate NAD^+-free cTSOX, the α(Gly139Ala) mutant was constructed. Expression of the mutant protein was found to be highly temperature dependent. No expression was detected under standard conditions (LB, 29 °C) but was observed at lower temperatures. Cell lysates from cells grown at the optimal temperature (15 °C) exhibited a specific activity that was 20% of that observed for wild-type extracts from cells grown at 29 °C.

The α(Gly139Ala) mutant, purified from cells grown at 15 °C, exhibited a specific activity (10.7 units min^{-1} mg^{-1}) similar to that of the wild type enzyme (see Table 3). Flavin analysis showed that the mutant enzyme contained approximately stoichiometric amounts of covalently bound FMN (0.8 mol/mol) and noncovalently bound FAD (1.1 mol/mol). To evaluate the NAD^+ content, a TCA extract was prepared and mixed with semicarbazide and ethanol, as described for the

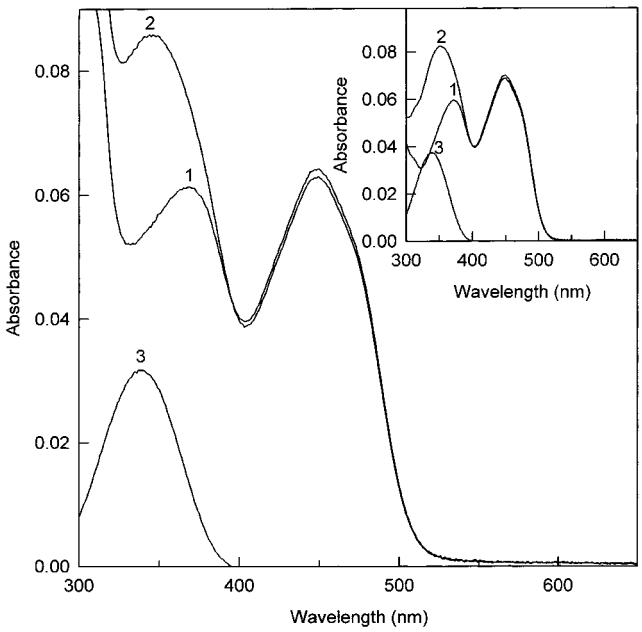

FIGURE 11: NAD^+ content of the α(Gly139Ala) mutant of cTSOX. Curve 1 is the absorption spectrum of the supernatant obtained after TCA precipitation and further treatment as described in the legend to Figure 7. Curve 2 was recorded 6 min after addition of yeast alcohol dehydrogenase (2.6 units/mL) at 25 °C. Curve 3 is the difference spectrum obtained by subtracting curve 1 from curve 2. The inset shows the corresponding data obtained with wild-type recombinant enzyme.

$\alpha\gamma$ complex. In this case, the extract contained the noncovalent FAD and exhibited a typical flavin spectrum (Figure 11, curve 1). Addition of yeast alcohol dehydrogenase resulted in an increase in absorbance in the 300−400 nm region (Figure 11, curve 2). The difference spectrum shows a peak at 340 nm (Figure 11, curve 3), as expected for the formation of NADH. The reaction with the mutant extract is very similar to that observed with wild-type cTSOX (Figure 11, inset). Calculations indicate that the mutant enzyme contained 1.0 mol of NAD^+/mol of protein.

The results show that NAD^+ is tightly bound to the α-(Gly139Ala) mutant and not lost during enzyme purification at 4 °C. Loss of NAD^+ has been observed upon incubation of the wild-type enzyme at elevated temperatures (e.g., ∼50% loss after 30 min at 37 °C) (*3*). To determine whether the α(Gly139Ala) mutation affected the stability of bound NAD^+, wild-type and mutant enzymes were incubated for 40 h at 25 °C and then for 24 h at 31 °C. Aliquots were withdrawn at various time points; free NAD^+ was determined using yeast alcohol dehydrogenase, which does not react with cTSOX-bound NAD^+ (*3*). The same rate of NAD^+ release was observed for wild-type and mutant cTSOX (data not shown).

As compared with a Gly → Ala mutation, a much larger decrease in nucleotide binding affinity would be expected upon mutation of α(Gly139) to Val, as judged by results obtained with other $NAD(P)^+$-binding proteins (*28*). However, no expression was detected with the α(Gly139Val) cTSOX mutant when cells were grown in LB medium at 29, 25, 15, 10, or 3 °C.[4]

Mutation of β(Gly30) to Ala. The observed stoichiometric binding of NAD^+ to the α subunit strongly suggests that the FAD site is likely to involve the second ADP-binding

motif near NH_2 terminus of the β subunit. In an effort to isolate FAD-free cTSOX, the second glycine in the ADP-binding motif of the β subunit (GX**G**^{30}XXG) was changed to alanine. The β(Gly30Ala) mutant was not expressed when cells were grown under standard conditions (LB, 29 °C), as judged by native or SDS−PAGE analysis of cell lysates. Extracts from cells grown on tryptone−phosphate medium at 25 °C exhibited wild-type expression levels of all four subunits. The subunits did not undergo normal assembly since a band that comigrated with the wild-type enzyme was not detected upon native gel electrophoresis. The β-(Gly30Ala) mutant expression patterns (data not shown) are virtually identical to those observed with the β(His173Ala) mutant (see Figure 4) where covalent flavinylation was blocked by mutating the FMN attachment site. This similarity suggested that the β(Gly30Ala) mutation might also prevent covalent attachment of FMN. To test this hypothesis, SDS gels were overloaded with protein (90 μg of soluble extract per lane) and examined under UV light prior to being stained for protein. Under these conditions, the β subunit in wild-type lysates exhibits a yellow fluorescence due to covalent FMN. The β subunit in the mutant extract was nonfluorescent, indicating that the β(Gly30Ala) mutation also blocks covalent flavinylation.

Attempted Expression of the β Subunit by Itself. Two constructs were developed in an effort to express the β subunit from cTSOX by itself. In plasmids pLJC305ΔBsmI and pET-β, expression of the gene coding for the β subunit (*soxB*) was placed under the control of the *lac* and T7 promoters, respectively. No expression of the β subunit was observed with either construct using *E. coli* XL-1 Blue or *E. coli* BL21(DE3) as host cell, respectively, as judged by SDS−PAGE or Western blot analysis. Growth conditions tested included different media (LB, tryptone−phosphate) and temperatures (15, 20, 25, and 29 °C).

Reaction of pTSOX with Sulfite. Various results suggest that FAD binds noncovalently to the β subunit of TSOX in a manner otherwise analogous to that observed for the covalently bound FAD in MSOX and MTOX. The β subunit of TSOX exhibits sequence similarity with MSOX and MTOX. An NH_2-terminal ADP-binding motif is present in all three polypeptides and forms part of the coenzyme binding site in MSOX. Residues which bind sarcosine in MSOX are conserved in the β subunit. The single sarcosine binding site in cTSOX is located near FAD, the flavin that acts as the immediate electron acceptor from sarcosine in TSOX, MSOX, and MTOX (*8*, *11*, *14*). Given this scenario, the environment and reactivity of the noncovalent FAD in TSOX should resemble that observed for the covalent FAD in MSOX and MTOX.

Formation of a reversible covalent complex involving nucleophilic addition of sulfite at flavin N(*5*) is a feature characteristic of flavoprotein oxidases and not generally observed with other classes of flavoenzymes (*30*). Sulfite complex formation is observed with MSOX and MTOX, but the reaction is orders of magnitude slower than observed with other flavoprotein oxidases (*11*, *31*). Our previous studies with cTSOX led us to conclude that only the covalent FMN forms a complex with sulfite (*23*). However, the recently observed slow reaction of MSOX and MTOX with sulfite raised the possibility that a comparable reaction with the FAD in cTSOX may have been overlooked, particularly since the reaction with the covalent FMN occurs immediately upon mixing with sulfite.

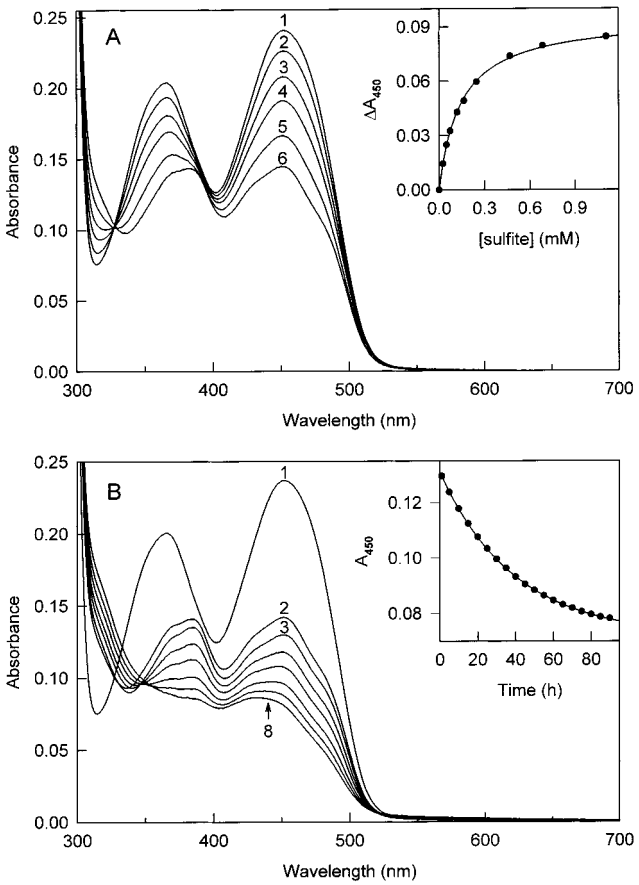

FIGURE 12: Reaction of pTSOX with sulfite. The recombinant enzyme was treated with H_2O_2 to disrupt the 4a-adduct, as described in the footnote to Table 4. Panel A shows a titration of the enzyme with sulfite in 45 mM potassium phosphate buffer, pH 8.0 at 25 °C. Curves 1−6 were recorded immediately after addition of 0.0, 0.025, 0.073, 0.164, 0.469, and 58.6 mM sulfite, respectively. The inset to panel A shows a fit (solid line) of the titration data (filled circles) to a hyperbolic saturation curve [$\Delta A_{obs} = \Delta A_{max}$[sulfite]/([sulfite] + K_d)]. Panel B shows the spectral course of the reaction of pTSOX with 150 mM sulfite in 40 mM potassium phosphate buffer, pH 8.0 at 4 °C. Curves 1 and 2 were recorded before and immediately after addition of sulfite, respectively. Curves 3−8 were recorded after incubation for 1, 10, 20, 35, 50, and 70 h, respectively. The inset shows a fit (solid line) of the data (filled circles) for the slow reaction to a single-exponential expression ($A_{obs} = \Delta A_{max}e^{-kt} + A_{final}$).

The sulfite reaction was reexamined in studies with pTSOX after the 4a-adduct in the isolated recombinant enzyme was disrupted with H_2O_2. Titration of pTSOX results in the immediate formation of a sulfite complex with about half of the flavin, as judged by the 40% bleaching of the absorbance at 450 nm (Figure 12A), similar to that observed with recombinant cTSOX (42%) or the natural corynebacterial enzyme (45−48%) (*10*, *23*). The titration data with pTSOX give a good fit to a theoretical binding curve (Figure 12A, inset) with an estimated dissociation constant (K_d = 143 ± 2 μM) similar to that observed for the reaction of sulfite with the covalent FMN in cTSOX (K_d = 260 μM) (*8*) under the same reaction conditions (pH 8.0, 25 °C).

To investigate a possible slow reaction with the noncovalent FAD, spectral changes were monitored after pTSOX was mixed with 150 mM sulfite under the same conditions except that the temperature was lowered to 4 °C to enhance

the long-term stability of the enzyme. Consistent with the titration study, 40% bleaching of the absorbance at 450 nm was observed immediately after sulfite addition (Figure 12B, curve 2). A second reaction was, indeed, observed upon further incubation that resulted in the bleaching of 70% of the initial absorbance at 450 nm (Figure 12B, curves 3−8). The slow reaction exhibited apparent first-order kinetics (Figure 12B, inset) [$k_{obs} = (25.4 \pm 0.2) \times 10^{-3}$ h^{-1}]. The results show the noncovalent FAD in pTSOX forms a sulfite complex in a slow reaction, similar to that observed with MTOX and MSOX. The observed reaction of sulfite with both flavins in pTSOX suggests that caution must be exercised in attempting to simplify the reductive half-reaction kinetics by assuming that sulfite will only react with the covalent FMN (*26*).

Reaction of pTSOX with Methylthioacetate. MSOX and MTOX form charge transfer complexes with methylthioacetate (MTA), a substrate analogue where the amino nitrogen in sarcosine is replaced by sulfur (*11*, *31*). If the noncovalent FAD in TSOX is equivalent to the covalent FAD in MSOX and MTOX, TSOX would be expected to form a similar charge transfer complex involving the noncovalent FAD. Titration of pTSOX with MTA shows that the compound does indeed form a charge transfer complex, as judged by the development of a new absorption band at longer wavelengths (Figure 13A). The charge transfer band is not well resolved in the absolute spectrum owing to overlap with the red edge of the flavin absorption spectrum. The position of this band ($\lambda_{max} = 512$ nm) was estimated from the difference spectrum (Figure 13B, curve 1). The dissociation constant ($K_d = 4.7 \pm 0.1$ mM) was determined by fitting the titration data to a theoretical binding curve (Figure 13A, inset). The properties observed for the pTSOX·MTA complex are similar to those observed for the corresponding complexes with MSOX and MTOX (Table 5).

To determine whether the pTSOX·MTA complex involved the noncovalent FAD, the enzyme was mixed with 10 mM sulfite and then titrated with MTA. The sulfite concentration used in this experiment was sufficient to quantitatively complex the covalent FMN whereas negligible reaction could occur with the noncovalent FAD, particularly during the short time (20 min) required for the MTA titration. Complexing the covalent FMN with sulfite did not significantly affect the difference spectrum observed for the pTSOX·MTA complex (Figure 13B, curve 2) as compared to that observed in the absence of sulfite (Figure 13B, curve 1) and caused only a small increase in the dissociation constant ($K_d = 7.9 \pm 0.2$ mM). The results show that the MTA charge transfer complex involves the noncovalent FAD in pTSOX.

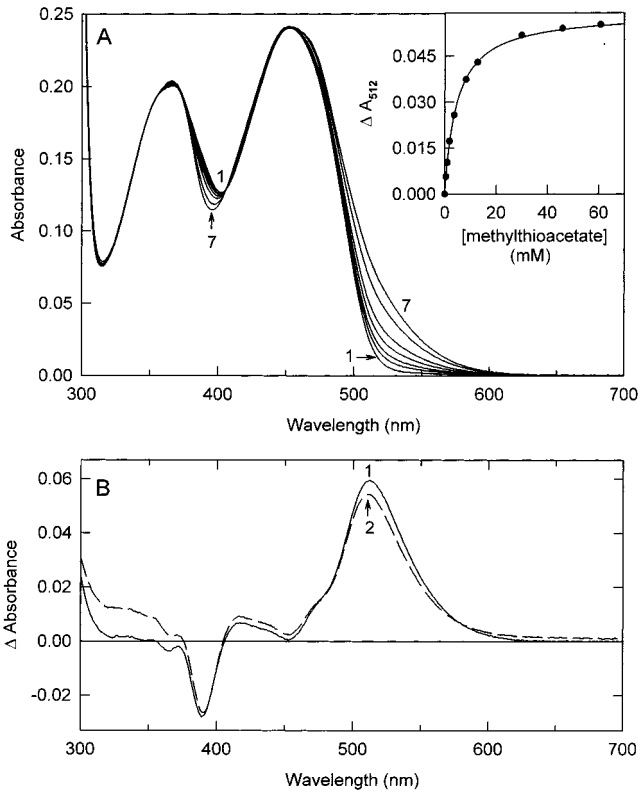

FIGURE 13: Reaction of pTSOX with methylthioacetate (MTA). The recombinant enzyme was treated with H_2O_2 to disrupt the 4a-adduct, as described in the footnote to Table 4. Panel A shows a titration of the enzyme with MTA in 50 mM potassium phosphate buffer, pH 8.0 at 25 °C. Curves 1−7 were recorded immediately after addition of 0.0, 0.50, 0.98, 1.92, 3.70, 12.7, and 106 mM MTA, respectively. The inset to panel A shows a fit (solid line) of the titration data (filled circles) to a hyperbolic saturation curve [$\Delta A_{obs} = \Delta A_{max}[MTA]/([MTA] + K_d)$]. Panel B: Curves 1 and 2 show difference spectra for the MTA complex determined in the absence or presence of 10 mM sulfite, respectively. Spectra were normalized to 100% complex formation using the measured complex dissociation constants and the spectral data obtained at the highest ligand concentration tested (106 mM). Curve 2 was also normalized to the same initial concentration of MSOX used in the titration in the absence of sulfite.

Table 5: Comparison of pTSOX·MTA, MSOX·MTA, and MTOX·MTA Charge Transfer Complexes[a]

enzyme	λ_{max} (nm)	K_d (mM)
pTSOX	512	4.7
MSOX	532	2.6
MTOX	516	32.3

[a] The complex with pTSOX involves the noncovalent FAD, as described in the text. Values for MSOX (*11*) and MTOX (*31*) are as previously reported.

DISCUSSION

Role of the Covalent Flavin Linkage. Insight regarding the function of the covalent bond between the 8α-position of FMN and His173 in the β subunit of cTSOX was obtained by mutating this residue to Asn. The β(His173Asn) mutant exhibits apparently normal subunit expression and assembly, as judged by native, SDS−PAGE, and Western blot analysis of mutant cell lysates. The mutant heterotetramer is, however, catalytically inactive and considerably less stable than wild-type cTSOX. The β and δ subunits are lost from the mutant enzyme during purification, which yields a nearly pure, flavin-free, complex containing the α and γ subunits in a 1:1 stoichiometry. The addition of possible stabilizing agents (glycerol, FMN, FAD) to buffers used during purification prevents loss of the δ subunit but not the β subunit, resulting in the isolation of a flavin-free $\alpha\gamma\delta$ complex.

The results show that the covalent flavin link is a critical structural element in TSOX. The β subunit is the least stable subunit in the mutant heterotetramer. Loss of the β subunit appears to weaken the interaction between the δ subunit and the $\alpha\gamma$ complex, as judged by the observed instability of the $\alpha\gamma\delta$ complex in the absence of external stabilizing agents. Recent studies show that the covalent flavin link has an

important structural function in monoamine oxidase A. The mutant enzyme is very unstable when removed from the outer mitochondrial membrane whereas wild-type monoamine oxidase A can be solubilized in a stable form (*32*). A structural role for the covalent link is not, however, a universal property, as judged by results obtained with other enzymes [vanillyl alcohol oxidase (*33*, *34*), fumarate reductase (*35*), succinate dehydrogenase (*36*)] where the mutant forms exhibit stability and structural properties similar to those of the corresponding wild-type enzymes. The fumarate reductase and succinate dehydrogenase data are of particular interest because these heterotetrameric enzymes exhibit a complex quaternary structure and contain multiple redox centers, analogous to that observed with TSOX.

The covalent flavin link in TSOX may also be essential for catalysis, as judged by the absence of TSOX activity in β(His173Asn) cell lysates that contain the intact, mutant heterotetramer. This proposal, however, assumes that the intact heterotetramer contains noncovalently bound FMN in place of the covalently bound FMN present in the wild-type enzyme. If this assumption is incorrect, the results would suggest that the covalent link in TSOX plays a key role in preventing FMN loss. In studies with monoamine oxidase A (*32*), succinate dehydrogenase (*36*), fumarate reductase (*35*), vanillyl alcohol oxidase (*33*, *34*), and trimethylamine dehydrogenase (*37*), the mutant enzymes were found to contain noncovalently bound flavin and exhibit significant catalytic activity, albeit at reduced levels as compared with the wild-type enzyme. The tight binding observed for the noncovalent flavin in the mutant forms of vanillyl alcohol oxidase and monoamine oxidase A has led some workers (*32*) to reject a possible role of the covalent flavin link in preventing flavin loss. Indeed, the numerous noncovalent interactions between FAD and the protein in MSOX (*14*) led us to predict that loss of the covalent link would yield a mutant enzyme containing noncovalently bound FAD. However, FAD binds very weakly to the mutant form of MSOX, which is isolated as an apoenzyme that exhibits catalytic activity when assayed in the presence of excess FAD ($K_{d\ app} = 2 \times 10^{-4}$ M).[3] The results clearly show that the covalent flavin link can play an important role in preventing flavin loss in some enzymes. Overall, the findings indicate a diversity of function for the covalent flavin link in different proteins. The current TSOX data do not allow us to distinguish between the two possible explanations for the total lack of activity in cell lysates that contain the intact, mutant heterotetramer. However, we suspect that FMN binds weakly to the mutant enzyme and that loss of FMN yields an unstable apoenzyme that undergoes irreversible denaturation.

The Covalent FMN Binding Site. About half of the covalent FMN in preparations of recombinant TSOX from *Corynebacterium* sp. P-1 and *P. maltophilia* is present as a reversible covalent 4a-adduct with a cysteine residue. In vitro studies show that the adduct is irreversibly disrupted by turnover with sarcosine or reaction with H_2O_2 (*10*). The adduct is not found in the corresponding natural enzymes probably because the adduct is disrupted in vivo by reaction with sarcosine which is used to induce expression of the natural but not the recombinant enzymes. Adduct formation was not prevented by mutating any of the three cysteine residues in the β subunit of cTSOX to Ser or Ala. The results show that the β subunit does not contain the reactive cysteine. Since the covalent FMN is attached via its 8-methyl group to the β subunit, this finding indicates that the flavin ring is located at the interface between β and another subunit that contains the reactive cysteine residue.

On the basis of the results obtained with cTSOX and pTSOX, we postulate that the 4a-adduct is a general property of recombinant TSOX and is an intermediate in the biosynthesis of the heterotetramer that is subsequently consumed during turnover of the newly synthesized enzyme with sarcosine. In this case, the reactive cysteine that forms the 4a-adduct should be a highly conserved residue. The δ subunit contains three absolutely conserved cysteine residues, as judged by multiple sequence analysis of five different heterotetrameric sarcosine oxidases. No conserved cysteine residues were found upon comparison of the corresponding α, β or γ subunits.[5] Interaction between the β and δ subunits is consistent with results obtained with the β(His173Asn) mutant where dissociation of the β subunit appeared to weaken the interaction between the δ subunit and the $\alpha\gamma$ complex. The data suggest that the β subunit in the wild-type enzyme binds to both the δ subunit *and* the $\alpha\gamma$ complex and thereby stabilizes the association of δ with the $\alpha\gamma$ complex. 4a-Thiolate adducts are formed as catalytic intermediates in flavoenzymes with redox-active disulfides (*38*) and probably during the photocycle of a plant blue light receptor (*39*). The postulated role of the 4a-adduct as an intermediate in the biosynthesis of an oligomeric enzyme is novel and currently under investigation.

Role and Binding Site of NAD$^+$ in TSOX. The α and β subunits each contain an NH_2-terminal ADP-binding motif that could serve as part of the binding site for FAD or NAD^+ in the wild-type enzyme. The flavin-free $\alpha\gamma$ complex was found to contain 1 mol of NAD^+, implicating the α subunit as the binding site for NAD^+. Definitive evidence was obtained by expressing the α subunit from cTSOX by itself and showing that the purified subunit contained 1 mol of NAD^+/mol of protein.

Our studies have shown that NAD^+ is not reduced by sarcosine or in redox equilibrium with the flavins. NAD^+ is tightly bound to the wild-type enzyme; attempts to selectively remove the coenzyme were not successful (*3*). The ADP-binding motif near the N-terminus of the α subunit contains three highly conserved glycine residues (GX**G**^{139}XXG). In an attempt to generate NAD^+-free cTSOX, α(Gly139) was mutated to Ala or Val. The Gly $\rightarrow$ Ala mutation drastically affects cTSOX expression, which was detected only in lysates from cells grown at low temperature. The α(Gly139Ala) mutant enzyme (isolated from cells grown at 15 °C) was found to contain 1 mol each of NAD^+, FAD, and covalent FMN and to exhibit catalytic properties and NAD^+ binding affinity similar to those of the wild-type enzyme. The slower rate of protein synthesis at the low temperature required for expression of the α(Gly139Ala) mutant may facilitate incorporation of NAD^+ into the mutated binding site. However, once NAD^+ incorporation has occurred, the properties of the mutant enzyme are essentially indistinguishable from those of the wild-type enzyme. As compared with the Gly $\rightarrow$ Ala mutation, a much larger decrease in nucleotide

[5] M. S. Jorns, unpublished results.

binding affinity would be expected upon mutation of α(Gly139) to Val, as judged by results obtained with other NAD(P)$^+$-binding proteins (*28*). No expression of the α-(Gly139Val) mutant was detected, even at temperatures as low as 3 °C. In this case, slowing the rate of protein synthesis is apparently insufficient to overcome the much larger barrier to NAD$^+$ binding. The results suggest that binding of NAD$^+$ to the α subunit is important for cTSOX expression, probably due to its effect on the folding and/or stability of the α subunit.

FAD Binding Site and Properties of TSOX-Bound FAD. Since the α subunit bound NAD$^+$, the FAD-binding site was likely to involve the ADP-binding motif near the NH_2 terminus of the *β* subunit, as observed for the covalently bound FAD in MSOX (*14*). The second glycine in the ADP-binding motif in the *β* subunit (GX**G**^{30}XXG) was changed to alanine in an attempt to generate FAD-free cTSOX. Although wild-type subunit expression levels were observed in lysates from cells grown in rich medium at reduced temperature, the *β*(Gly30Ala) mutation was found to block both subunit assembly *and* covalent flavinylation of the *β* subunit. The results suggest that the noncovalent binding of FAD to the *β* subunit in the wild-type enzyme triggers a conformational change that is required for covalent FMN attachment and subunit assembly. Attempts to express the wild-type *β* subunit by itself were unsuccessful, suggesting that one (or more) of the other subunits may be needed for the *β* subunit to achieve a stable conformation. This scenario is consistent with the finding that the covalent FMN in *β* is bound at a subunit interface. Unlike the *β* subunit, the α subunit can fold into an apparently stable native conformation when expressed by itself, as judged by the observed stoichiometric incorporation of tightly bound NAD$^+$.

Although we could not obtain definitive evidence to show that the noncovalent FAD binds to the *β* subunit, the proposed binding site is supported by various other observations, including the observed sequence similarity of the *β* subunit with MSOX and MTOX (especially the conservation of residues that bind sarcosine) and the presence of a single binding site in cTSOX near the noncovalent FAD, the flavin that serves as the immediate electron acceptor from sarcosine (*8*, *11*, *14*). Given this scenario, it was predicted that the environment and reactivity of the noncovalent FAD in TSOX would resemble that observed for the covalent FAD in MSOX and MTOX. This postulate is consistent with results obtained for the reaction of the noncovalent FAD in cTSOX with sulfite and methylthioacetate. Formation of a covalent sulfite complex with the noncovalent FAD in cTSOX is extremely slow, unlike the rapid reactions observed with most other flavoprotein oxidases, but similar to the very slow reactions observed with MSOX and MTOX (*11*, *31*). The sarcosine analogue, methylthioacetate, forms similar charge transfer complexes with the noncovalent FAD in pTSOX and with the covalent FAD in MSOX or MTOX, as judged by the position of the charge transfer bands and the stability of the complexes (see Table 5).

TSOX Model. In our working model (Figure 14), we propose that FAD binds noncovalently to the *β* subunit with an entry channel for sarcosine above the *re* face of the flavin ring, analogous to the binding mode observed for the covalently bound FAD in MSOX (*14*). The covalent attachment site for FMN in the *β* subunit (His173) aligns with

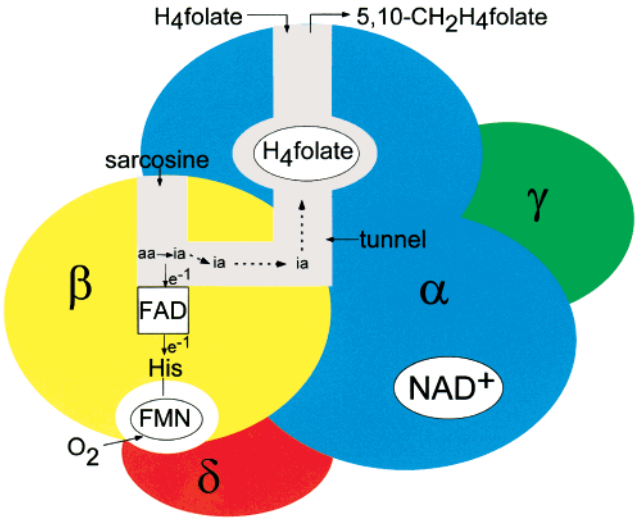

FIGURE 14: TSOX model. aa and ia refer to sarcosine and its corresponding imine, respectively. The symbol, e^{-1}, is used to represent electron transfer from sarcosine to FAD and then to FMN.

Ser149 in MSOX. The hydroxyl group of Ser149 in MSOX is located in a small depression on the protein surface, about 8 Å above the *si* face of the FAD ring (*14*). We therefore propose that FMN is covalently attached to the side of the *β* subunit opposite to the sarcosine entry channel. The resulting separation between the flavin rings is reasonably consistent with other studies which indicate that the flavins in TSOX must be at least 10 Å apart (*8*, *9*). The FMN ring in TSOX is located at the interface between *β* and a subunit which contains the cysteine residue that forms a 4a-thiolate adduct with FMN. The *δ* subunit is tentatively assigned to this subunit interface since it contains the three absolutely conserved cysteine residues found in TSOX from various sources. The postulated interaction between the *β* and *δ* subunits could also account for results which suggest that the *β* subunit stabilizes the interaction between the *δ* subunit and the α*γ* complex. A two-domain structure is proposed for the α subunit, consistent with sequence analysis studies (*2*). NAD$^+$ binds to the ADP-binding motif in the NH_2-terminal domain. Preliminary results indicate that the isolated α subunit binds H_4folate.[6] We propose that H_4folate binds to the COOH-terminal domain, which exhibits sequence homology with other enzymes that bind H_4folate and catalyze the formation of 5,10-CH_2-H_4folate, using different 1-carbon donors (*2*). In the presence of H_4folate, sarcosine oxidation is efficiently coupled to the synthesis of 5,10-CH_2-H_4folate with the sarcosine imine as the probable 1-carbon donor (*6*, *7*). Efficient coupling of two reactions involving a hydrolytically labile intermediate might be accomplished by substrate channeling (*40*), as suggested in the model where the flavin and folate sites are connected by a tunnel with restricted solvent access. Alternatively, efficient coupling may involve juxtaposition of the two catalytic sites to form a composite active site. The *γ* subunit does not contain any identifiable motifs or exhibit sequence homology with any other protein. It is proposed that the *γ* subunit binds only to the α subunit and does not interact with the *β* or *δ* subunits, a model consistent with the fact that the α and *γ* subunits can form a stable 1:1 complex.

[6] P. Khanna and M. S. Jorns, unpublished results.

REFERENCES

1. Kvalnes-Krick, K., and Jorns, M. S. (1991) in *Chemistry and Biochemistry of Flavoenzymes* (Muller, F., Ed.) pp 425−435, CRC Press, Inc., Boca Raton, FL.
2. Chlumsky, L. J., Zhang, L., and Jorns, M. S. (1995) *J. Biol. Chem. 270*, 18252−18259.
3. Willie, A., and Jorns, M. S. (1995) *Biochemistry 34*, 16703−16707.
4. Willie, A., Edmondson, D. E., and Jorns, M. S. (1996) *Biochemistry 35*, 5292−5299.
5. Chlumsky, L. J., Sturgess, A. W., Nieves, E., and Jorns, M. S. (1998) *Biochemistry 37*, 2089−2095.
6. Wagner, M. A., and Jorns, M. S. (1997) *Arch. Biochem. Biophys. 342*, 176−181.
7. Kvalnes-Krick, K., and Jorns, M. S. (1987) *Biochemistry 26*, 7391−7395.
8. Zeller, H.-D., Hille, R., and Jorns, M. S. (1989) *Biochemistry 28*, 5145−5154.
9. Ali, S. N., Zeller, H. D., Calisto, M. K., and Jorns, M. S. (1991) *Biochemistry 30*, 10980−10986.
10. Chlumsky, L. J., Zhang, L. N., Ramsey, A. J., and Jorns, M. S. (1993) *Biochemistry 32*, 11132−11142.
11. Wagner, M. A., Trickey, P., Chen, Z., Mathews, F. S., and Jorns, M. S. (2000) *Biochemistry 39*, 8813−8824.
12. Wagner, M. A., and Jorns, M. S. (2000) *Biochemistry 39*, 8825−8829.
13. Wagner, M. A., Khanna, P., and Jorns, M. S. (1999) *Biochemistry 38*, 5588−5595.
14. Trickey, P., Wagner, M. A., Jorns, M. S., and Mathews, F. S. (1999) *Structure 7*, 331−345.
15. Reuber, B. E., Karl, C., Reimann, S. A., Mihalik, S. J., and Dodt, G. (1997) *J. Biol. Chem. 272*, 6766−6776.
16. Koyama, Y., and Ohmori, H. (1996) *Gene 181*, 179−183.
17. Ho, S. N., Hunt, H. D., Horton, R. M., Pullen, J. K., and Pease, L. R. (1989) *Gene 77*, 51−59.
18. Ausubel, F. M., Brent, R., Kingston, R. E., Moore, D. D., Seidmen, J. G., Smith, J. A., and Struhl, K. (1989) *Current Protocols in Molecular Biology*, John Wiley & Sons, New York.
19. Moore, J. T., Uppal, A., Maley, F., and Maley, G. F. (1993) *Protein Expression Purif. 4*, 160−163.
20. Bradford, M. (1976) *Anal. Biochem. 72*, 248−255.
21. Suzuki, M. (1981) *J. Biochem. 89*, 599−607.
22. Nash, T. (1953) *Biochem. J. 55*, 416−421.
23. Jorns, M. S. (1985) *Biochemistry 24*, 3189−3194.
24. Kvalnes-Krick, K., and Jorns, M. S. (1986) *Biochemistry 25*, 6061−6069.
25. Weber, K., and Osborn, M. (1969) *J. Biol. Chem. 244*, 4406−4412.
26. Harris, R. J., Meskys, R., Sutcliffe, M. J., and Scrutton, N. S. (2000) *Biochemistry 39*, 1189−1198.
27. Davis, J. P., and Copeland, R. A. (1997) *Biochem. Pharmacol. 54*, 459−465.
28. Rescigno, M., and Perham, R. N. (1994) *Biochemistry 33*, 5721−5727.
29. Morandi, P., Valzasina, B., Colombo, C., Curti, B., and Vanoni, M. A. (2000) *Biochemistry 39*, 727−735.
30. Massey, V., Muller, F., Feldberg, R., Schuman, M., Sullivan, P. A., Howell, L. G., Mayhew, S. G., Matthews, R. G., and Foust, G. P. (1969) *J. Biol. Chem. 244*, 3999−4006.
31. Khanna, P., and Jorns, M. S. (2001) *Biochemistry 40*, 1441−1450.
32. Nandigama, R. K., and Edmondson, D. E. (2000) *J. Biol. Chem. 275*, 20527−20532.
33. Fraaije, M. W., van den Heuvel, R. H. H., Van Berkel, W. J. H., and Mattevi, A. (1999) *J. Biol. Chem. 274*, 35514−35520.
34. Fraaije, M. W., van den Heuvel, R. H. H., van Berkel, W. J. H., and Mattevi, A. (2000) *J. Biol. Chem. 275*, 38654−38658.
35. Blaut, M., Whittaker, K., Valdovinos, A., Ackrell, B. A. C., Gonsalus, R. P., and Cecchini, G. (1989) *J. Biol. Chem. 264*, 13599−13604.
36. Robinson, K. M., Rothery, R. A., Weiner, J. H., and Lemire, B. D. (1994) *Eur. J. Biochem. 222*, 983−990.
37. Scrutton, N. S., Packman, L. C., Mathews, F. S., Rohlfs, R. J., and Hille, R. (1994) *J. Biol. Chem. 269*, 13942−13950.
38. Williams, C. H. (1992) in *Chemistry and Biochemistry of Flavoenzymes* (Muller, F., Ed.) Vol. III, pp 121−211, CRC Press, Boca Raton, FL.
39. Salomon, M., Christie, J. M., Knieb, E., Lempert, U., and Briggs, W. R. (2000) *Biochemistry 39*, 9401−9410.
40. Miles, E. W., Rhee, S., and Davies, D. R. (1999) *J. Biol. Chem. 274*, 12193−12196.

BI010101P